### 1

# The Importance of Astrophysical Distance Measurements

When we try to pick out anything by itself, we find it hitched to everything else in the Universe.

– John Muir (1838–1914), American naturalist and explorer

Each problem that I solved became a rule, which served afterwards to solve other problems.

- René Descartes (1596–1650), French philosopher

Accurate distance measurements are of prime importance for our understanding of the fundamental properties of both the Universe as a whole and the large variety of astrophysical objects contained within it. But astronomical distance measurement is a challenging task: the first distance to another star was measured as recently as 1838, and accurate distances to other galaxies – even the nearest – date only to the 1950s, despite evidence of the existence of 'spiral nebulae' as early as Lord Rosse's observations in the mid-nineteenth century. This is not surprising, since the only information we have about any object beyond our solar system includes its position (perhaps as a function of time), its brightness (as a function of wavelength and time) and possibly its radial velocity and chemical composition.

While we can determine highly accurate distances to objects in our solar system using active radar measurements, once we leave the Sun's immediate environment, most distance measurements depend on inferred physical properties and are, therefore, fundamentally uncertain. Yet at the same time, accurate distance measurements on scales of galaxies and beyond are crucial to get a handle on even the most basic questions related to the age and size of the Universe as a whole as well as its future evolution. The primary approach to obtaining distance measurements at increasingly greater distances is by means of the so-called *distance ladder*, where – in its most simplistic form – each rung is calibrated using the rung immediately below it. It is, therefore, of paramount importance to reduce the

statistical uncertainties inherent to measuring distances to even the nearest star clusters in our Milky Way, because these objects are the key benchmarks for calibrating the cosmic distance scale locally. In this book, we take the reader on a journey from the solar neighbourhood to the edge of the Universe, *en passant* discussing the range of applicable distance measurement methods at each stage. Modern astronomers have developed methods of measuring distances which vary from the mundane (the astronomical equivalent of the surveyor's theodolite) to the exotic, such as the bending of light in **general relativity**<sup>1</sup> or using wiggles in the spectrum of the **cosmic microwave background** (CMB).

Not only do we provide an up-to-date account of the progress made in a large number of subfields in astrophysics, in turn leading to improved distance estimates, but we also focus in particular on the physics underlying the sometimes surprising notion that all of these methods work remarkably well and give reasonably consistent results. In addition, we point out the pitfalls one encounters in all of these areas, and particularly emphasize the state of the art in each field: we discuss the impact of the remaining uncertainties on a complete understanding of the properties of the Universe at large.

Before embarking on providing detailed accounts of the variety of distance measurement methods in use, here we will first provide overviews of some of the wide-ranging issues that require accurate determinations of distances, with appropriate forward referencing to the relevant chapters in this book. We start by discussing the distance to the Galactic Centre (Section 1.1). We then proceed to discuss the long-standing, although largely historical controversy surrounding the distance to the Large Magellanic Cloud (LMC) (Section 1.2). Finally, in Section 1.3 we go beyond the nearest extragalactic yardsticks and offer our views on the state of the art in determining the 3D structure of large galaxy clusters and large-scale structure, at increasing **redshifts**.

#### 1.1 The Distance to the Galactic Centre

The Galactic Centre hosts a dense, luminous star cluster with the compact, nonthermal radio source Sagittarius (Sgr) A\* at its core. The position of the latter object coincides with the Galaxy's kinematic centre. It is most likely a massive black hole with a mass of  $M_{\rm BH} \sim 4.4 \times 10^6 \ {\rm M_{\odot}}$  (see the review of Genzel et al. 2010), which is – within the uncertainties - at rest with respect to the stellar motions in this region. The exact distance from the Sun to the Galactic Centre, R<sub>0</sub>, serves as a benchmark for a variety of methods used for distance determination, both inside and beyond the Milky Way. Many parameters of Galactic objects, such as their distances, masses and luminosities, and even the Milky Way's mass and luminosity as a whole, are directly related to  $R_0$ . Most luminosity and many mass estimates scale as the square of the distance to a given object, while masses based on total densities or orbit modelling scale as distance cubed. This dependence sometimes involves adoption of a rotation model of the Milky Way, for which we also need to know the Sun's circular velocity with high accuracy. As the best estimate of R<sub>0</sub> is refined, so are the estimated distances, masses and luminosities of numerous Galactic and extragalactic objects, as well as our best estimates of the rate of Galactic rotation and size of the Milky Way. Conversely, if we could achieve a highly accurate *direct* distance determination to the Galactic Centre, this would allow reliable recalibration of the zero points of a range of secondary distance

<sup>&</sup>lt;sup>1</sup> Terms and concepts which appear in the Glossary are rendered in boldface font at first occurrence in the text.

calibrators, including **Cepheid**, **RR** Lyrae and **Mira variable stars** (Sections 3.5.2, 3.5.5 and 3.5.3, respectively), thus reinforcing the validity of the extragalactic distance scale (cf. Olling 2007). In turn, this would enable better estimates of globular cluster (GC) ages, the **Hubble constant** – which relates a galaxy's recessional velocity to its distance, in the absence of '**peculiar motions**' (see Section 5.1) – and the age of the Universe, and place tighter constraints on a range of cosmological scenarios (cf. Reid *et al.* 2009b).

#### 1.1.1 Early Determinations of $R_0$

The American astronomer, Harlow Shapley (1918a,b), armed with observations of GCs taken with the Mount Wilson 60-inch telescope (California, USA) since 1914, used the light curves of Cepheid variables and, hence, their **period–luminosity relation** to draw a map of the distribution of 69 GCs with respect to the Sun's position and the plane of the Milky Way (see Figure 1.1). He eventually extended this to include all 93 Galactic GCs known at the time. He concluded that the Sun was not located in or near the Galactic Centre—as previously deduced from star counts that were, in fact, heavily affected by interstellar **extinction** in the Galactic plane (e.g. Herschel 1785; Kapteyn 1922) — but at Galactic longitude  $\ell \simeq 325^{\circ}$  (in the direction of the constellation Sagittarius), at a distance of  $\sim 13-25$  kpc, i.e. significantly greater than the current best estimate of  $8.28 \pm 0.15 \pm 0.29$  kpc, where the two errors represent the statistical and systematic uncertainties (Genzel *et al.* 2010; see also Reid 1993; Eisenhauer *et al.* 2003; Horrobin *et al.* 2004; Ghez *et al.* 2008;

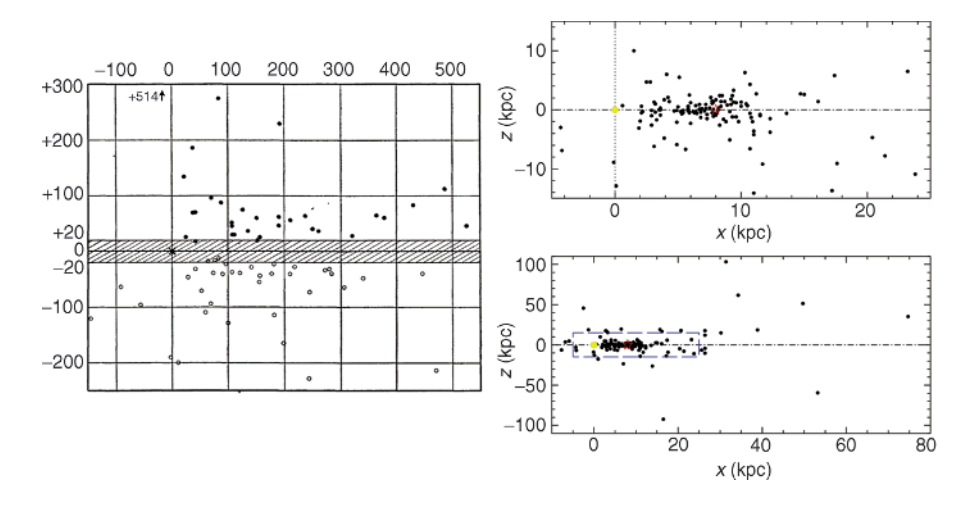


**Figure 1.1** (Left) Projection of the positions of globular clusters perpendicularly to the Galactic midplane (Shapley 1918a,b). Cross: position of the Sun. The unit of distance is 100 **parsec** (pc). The position of the GC NGC 4147 is indicated by the arrow (outside the figure boundaries). (Reprinted from H. Shapley and M. J. Reid, Astrophysical Journal, **48**, Studies based on the colors and magnitudes in stellar clusters. VII. The distances, distribution in space, and dimensions of 69 globular clusters, p. 154–181, Copyright 1918, with permission of the AAS.) (Right) Upto-date distribution of Galactic GCs (data collected by Harris 1996; 2010 edition). The Sun is located at the origin (indicated in yellow) and distances are based on RR Lyrae period-luminosity calibration (Section 3.5.5). The Galactic Centre is indicated by a red star. The blue dashed box in the bottom panel represents the area shown in the top panel.

#### 4 An Introduction to Distance Measurement in Astronomy

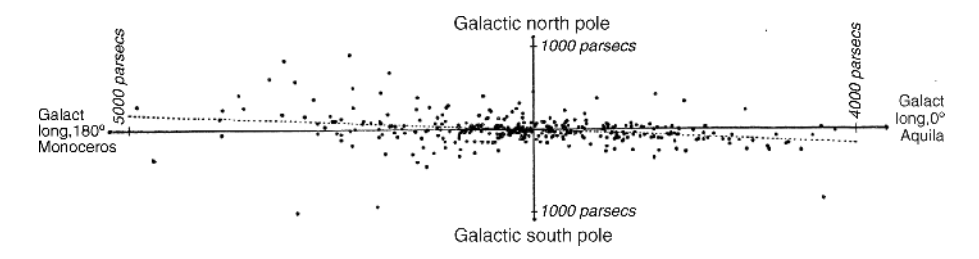


**Figure 1.2** Projection of Galactic open clusters on the same plane as in Figure 1.1 (Trumpler 1930). Dotted line: plane of symmetry of the open clusters. The Sun is located slightly to the left of the vertical axis, in the midst of a subset of open clusters shown as open circles (clusters within 1 kpc of the Sun). (Reprinted from R. J. Trumpler, Lick Observatory Bulletin, XIV, Preliminary results on the distances, dimensions, and space distribution of open star clusters, p. 154–188, Copyright 1930, with permission of UC Regents/Lick Observatory.)

Gillessen *et al.* 2009a; Majaess *et al.* 2009). He also found that the distribution of GCs above and below the Galactic plane was approximately symmetrical, with no clusters seen closer than 1300 pc from the plane.

Although Shapley's lower limit of  $R_0 \sim 13$  kpc is within a factor of 2 of the currently accepted value, his method of distance determination was affected by a number of partially compensating systematic errors. His Cepheid period–luminosity calibration was too faint by  $\sim 1$  mag, while he used 'Population II' Cepheids (**W Virginis stars**; see Section 3.5.4) instead of the type I Cepheids he thought he had observed. The former are generally some 2 mag fainter than the latter, leading to a distance scale that was  $\approx 1$  mag too bright and a distance overestimate by a factor of  $\sim 1.6$  (cf. Reid 1993).

By taking advantage of radial velocity and proper motion measurements tracing the differential rotation of stars in the solar neighbourhood – in the sense that stars closer to the Galactic Centre travelled faster than their counterparts at greater distances – the Dutch astronomer Jan Hendrik Oort (1927) established the centre of rotation about the Milky Way to within 2° of Shapley's estimate, at  $\ell=323^\circ$ . Note that this was at a much smaller distance, approximately 5.9 kpc, than Shapley's estimate. He adopted Lindblad's (1927) Galactic rotation model and assumed a circular velocity at the solar circle of  $v_c=272$  km s<sup>-1</sup>, which is now known to be considerably greater than International Astronomical Union recommendation of  $v_c=220$  km s<sup>-1</sup>.

The discrepancy between Shapley's and Oort's distance estimates to the Galactic Centre was predominantly caused by interstellar extinction, which was largely unknown at the time until Robert J. Trumpler's discovery of the effects of interstellar dust grains in the 1930s.<sup>3</sup> In 1929, Trumpler, a Swiss–American astronomer based at Lick Observatory (California, USA), tried to use open star clusters to repeat what Shapley had done with the Milky Way's GC population. He knew that open clusters tended to lie in the disc of the Galaxy and reasoned that this was a reasonable way to clarify the disc's shape (see Figures 1.2 and 1.3).

 $<sup>^2</sup>$  This would also have contributed to a smaller estimated distance to the Galactic Centre than that resulting from adoption of  $R_0=8.0$ –8.5 kpc, which is currently generally adopted and is in line with the International Astronomical Union recommendation of  $R_0=8.0$  kpc. Note that Reid *et al.* (2009a) recently obtained a revised best-fitting Galactic rotation velocity of  $v_c=254\pm16~km~s^{-1}$  based on a Galaxy-wide survey of masing sources in high-mass star-forming regions.

<sup>&</sup>lt;sup>3</sup> Although Trumpler is often credited with this discovery, its effects were first reported by Friedrich Georg Wilhelm von Struve in 1847.

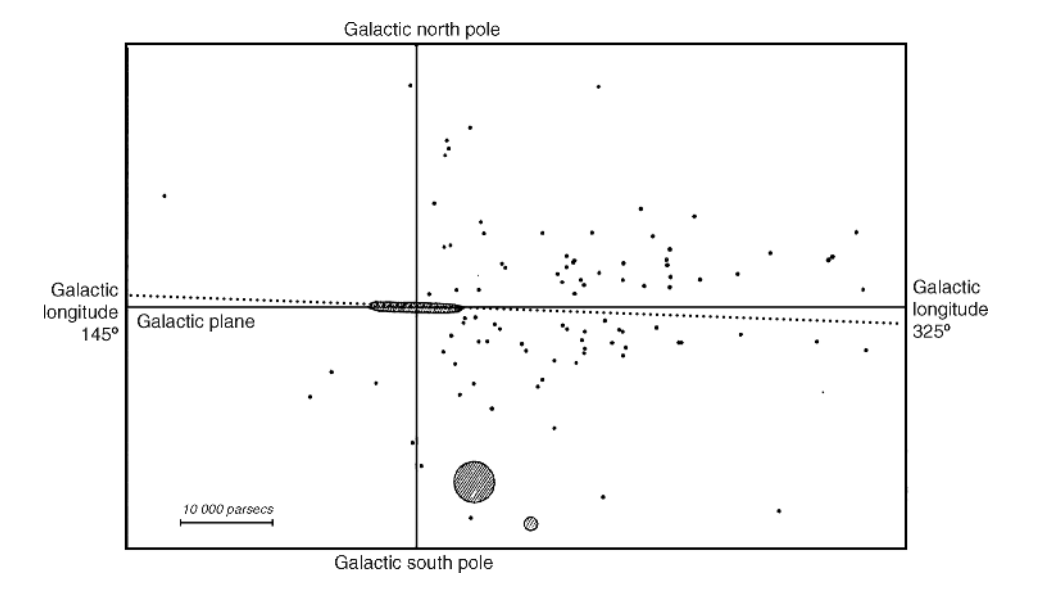


**Figure 1.3** Trumpler's (1930) view of the distribution of open and globular clusters in the Milky Way. Solid dots: GCs. Shaded area: open clusters (see Figure 1.2). Shaded circles: Magellanic Clouds. (Reprinted from R. J. Trumpler, Lick Observatory Bulletin, XIV, Preliminary results on the distances, dimensions, and space distribution of open star clusters, p. 154–188, Copyright 1930, with permission of UC Regents/Lick Observatory.)

Determining the distances to his sample of open clusters was key. Trumpler devised two ways to achieve this. First, he used a version of the **main-sequence fitting technique** (see Section 3.2.1) to estimate distances, in essence relying on the unproven principle of 'faintness equals farness', which was unproven in the sense that the idea had not been shown to work reliably. In an alternative technique, he deduced that if all open clusters had approximately the same physical, linear size, then the more distant ones would have smaller angular sizes, a 'smallness equals farness' argument. When he compared the results of both methods, he found that the main-sequence fitting technique gave systematically larger distances.

Unknowingly, Trumpler had stumbled on the evidence that the space between the stars is not entirely empty. Before Trumpler, it was known that there were obvious dark clouds in the sky which blocked the light from behind, such as the Coalsack Nebula. However, Trumpler showed that such effects were not confined to distinct clouds, but to a general 'fogginess' of space (see also Section 6.1.1). Its effect on the main-sequence fitting technique is to add a term, A, to the **distance modulus** equation to make the shift of the apparent magnitudes of Trumpler's clusters larger than they would have been in the absence of absorption:

$$m_V - M_V = 5\log(d/pc) - 5 + A_V,$$
 (1.1)

where  $m_V$  and  $M_V$  are the apparent and absolute magnitudes in the optical V filter, and d is the distance sought. Meanwhile, Trumpler's distance to the Galactic Centre, properly corrected for the effects of extinction, was actually very close to the present-day value. Note that because interstellar dust is most concentrated in the Galactic plane, Shapley's experiment with GCs was not affected, at least not significantly, by the interference of

absorption and scattering by dust. However, there is a clear lack of objects in his work in the direction of the Galactic midplane, where dust blocked his view and created the so-called 'zone of avoidance' for good GC targets.

Interestingly, Shapley commented that '... within 2000 parsecs of that plane there are only five [GCs], four of which are among the clusters nearest the sun.' Discussing the frequency distribution of his observed GCs as a function of distance from the Galactic plane, he notes that '[t]he completion of that curve, in a form naturally to be expected for the frequency of objects concentrated toward the Galaxy, would require at least 50 globular clusters within 1500 parsecs of the plane; there is, however, only one, Messier 22, ...' and '[h]ence we conclude that this great mid-galactic region, which is particularly rich in all types of stars, planetary nebulae, and open clusters, is unquestioningly a region unoccupied by globular clusters.'

#### 1.1.2 Modern Results

Since the presence of interstellar dust severely hampers our view of the Galactic Centre, longer-wavelength (IR and radio) observations (see e.g. Figure 1.4) have been employed extensively to arrive at more accurate Galactic Centre distance estimates. Reid (1993) and Genzel *et al.* (2010) provide extensive reviews of the range of methods used, as well as their accuracy at the time of these publications. In this section, we focus on the *primary, direct* methods of distance determination to the Galactic Centre (the reader is referred to Reid 1993, Genzel *et al.* 2010, as well as the relevant chapters elsewhere in this book for alternative methods) and summarize the current state of the art in this field.

Following Reid (1993), we distinguish the variety of methods used to determine  $R_0$  into primary, secondary and indirect measurements. Primary measurements determine  $R_0$ 

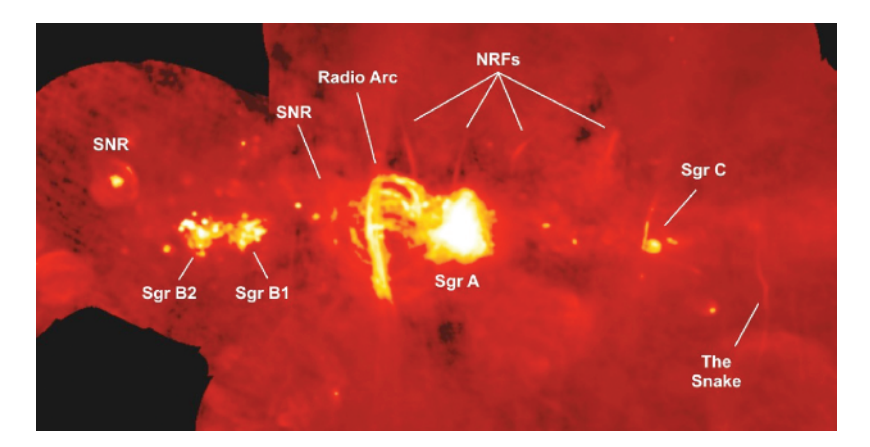


**Figure 1.4** Combined radio image, covering a range of radio wavelengths, of the Galactic Centre region based on observations obtained with the Very Large Array and the Green Bank Telescope. The horizontal and vertical coordinates represent Galactic longitude and latitude, respectively. The linear filaments near the top are nonthermal radio filaments (NRFs). SNR: supernova remnant. Sgr: Sagittarius. (Reprinted from Yusef-Zadeh et al., NRAO Press Release (Online), Origin of enigmatic Galactic Center filaments revealed, Copyright 2004, with permission of NRAO/AUI/NSF.)

directly, without having to rely on **standard candle** calibration (secondary methods) or a Galactic rotation model (one type of indirect method). The former include using proper motions and trigonometric parallax measurements of masing interstellar molecules (see also Section 3.7.4), OH/IR stars – late-type stars that exhibit 1612 MHz OH maser emission following far-IR 'pumping' of the population levels – near the Galactic Centre, direct Keplerian orbit measurements and statistical estimates based on assuming equality of radial and tangential (i.e. isotropic) velocity dispersions of the Galactic Centre star cluster. Secondary measurements include Shapley's method of using the centroid of the GC distribution - which is, in essence, based on adoption of a suitable period-luminosity relation for variable stars and assumes that the GC population is symmetrically distributed with respect to the Galactic Centre (see Reid 1993 and Figure 1.1 for a more recent update) – and of other, presumably symmetrically distributed, bright objects, and calibration based on RR Lyrae and Mira period-luminosity relations (cf. Section 3.5). In addition to these methods, indirect methods rely on either Galactic rotation models, the **Eddington luminosity** of X-ray sources (e.g. Reid 1993 and references therein) or the planetary nebula luminosity function (e.g. Dopita et al. 1992; see Section 4.4), among other endeavours (see also Vanhollebeke et al. 2009, their Table 1).

#### 1.1.2.1 Maser-Based Geometric Distances

The molecular material associated with massive stars at the time of starbirth is closely traced by water vapour. Population inversion of the  $\rm H_2O$  energy levels – which refers to a configuration with higher occupancy of excited than the lower energy states – by ionization caused by collisional pumping of the rotational energy levels and other shock-related physical processes (e.g. Elitzur 1992; Lo 2005) by the intense radiation from these massive stars and subsequent coherent de-excitation causes 22 GHz masing 'spots' to appear in the dust-rich envelopes of asymptotic giant branch stars, with sizes of  $\sim 10^{11}$  m and brightness temperatures<sup>5</sup> as high as  $10^{12}$ – $10^{15}$  K (cf. Reid 1993). These small sizes and high brightness temperatures render these objects ideal tracers for proper-motion measurements using **Very Long Baseline Interferometry** (VLBI) techniques (see also Section 3.7.4) because of the associated micro-arcsecond ( $\mu$ as) astrometric accuracy over fields of view of a few arcseconds in diameter.

Early geometric distance estimates to the Galactic Centre were based on the 'expanding cluster parallax' method (equivalent to the moving groups method; see Section 2.1.3) applied to two  $H_2O$  masers in the dominant, high-mass star-forming region near the Galactic Centre, Sgr B2, resulting in distances of 7.1 and between 6 and 7 kpc (Reid 1993) for Sgr B2 North<sup>6</sup> and Middle, respectively, with a combined statistical and systematic uncertainty of  $\pm 1.5$  kpc ( $1\sigma$ ). The accuracy attainable for distance determinations to  $H_2O$  maser sources is limited by (i) the motions of the individual spots (which exhibit random motions in all spatial coordinates of  $\approx 15$  km s<sup>-1</sup>, compared to typical measurement uncertainties of a few km s<sup>-1</sup>); (ii) their distribution around the exciting star: a nonuniform distribution, as observed for the Galactic Centre maser source Sgr B2 (North)

 <sup>4 &#</sup>x27;Masers' (microwave amplification by stimulated emission of radiation) are the microwave analogues of optical and IR lasers.
 5 The brightness temperature is the temperature of a blackbody in thermal equilibrium with its surroundings which resembles the observed intensity distribution of a 'grey-body' object at a given frequency.

<sup>&</sup>lt;sup>6</sup> Sgr B2 (North) is almost certainly located within 0.3 kpc of the Galactic Centre (Reid *et al.* 1988; Reid 1993; Snyder *et al.* 1994; Belloche *et al.* 2008). Reid *et al.* (2009b) derive a Galactocentric distance of 0.13 ± 0.06 kpc by adopting  $R_0 \approx 8.0$  kpc and  $v_{LSR,Sgr B2} \approx 62$  km s<sup>-1</sup> for the velocity of Sgr B2 with respect to the local standard of rest and a low-eccentricity orbit.

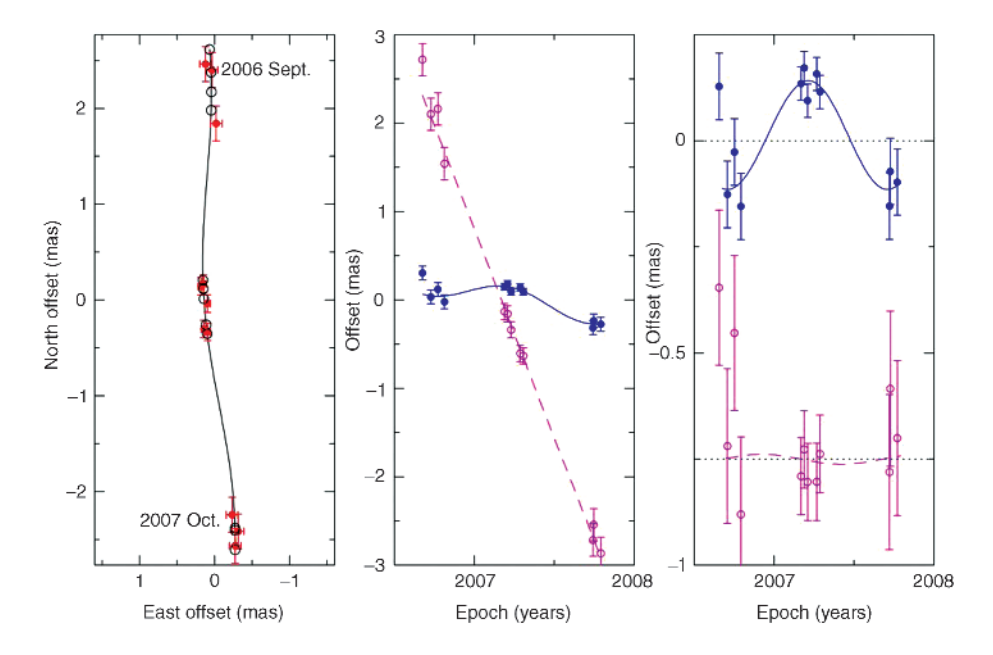


**Figure 1.5**  $H_2O$  maser parallax and proper-motion data and fits for Sgr B2N (Reid et al. 2009b). (Left) Positions on the sky (red circles). The expected positions from the parallax and proper motion fit are indicated (black circles and solid line, respectively). (Middle) East (filled blue circles and solid line) and North (open magenta circles and dashed line) position offsets and best-fitting parallax and proper motions as a function of time. (Right) Same as the middle panel, except the best-fitting proper motion has been removed, allowing the effects of only the parallax to be seen. (Reprinted from M. J. Reid et al., Astrophysical Journal, **705**, A trigonometric parallax of Sgr B2, p. 1548–1553, Copyright 2009, with permission of the AAS.)

(Reid *et al.* 1988), combined with the requirement to determine the line-of-sight distance from the central star for each spot, results in correlations between the maser source's expansion speed and its distance (cf. Reid 1993); and (iii) tropospheric signal propagation delays after calibration (cf. Reid *et al.* 2009b).

Reid *et al.* (2009b) recently provided the first trigonometric parallax measurement for the Galactic Centre (see Figure 1.5), using  $H_2O$  maser astrometry with the Very Long Baseline Array (VLBA), the US VLBI network. Their measured parallax for Sgr B2 (North) and Sgr B2 (Middle) is  $0.128 \pm 0.015$  and  $0.130 \pm 0.012$  milli-arcseconds (mas), respectively, leading to a combined parallax for the Sgr B2 region of  $0.129 \pm 0.012$  mas and, thus,  $R_0 = 7.8^{+0.8}_{-0.7}$  kpc. Correcting for the small offset between Sgr B2 and Sgr A\* (Sgr B2 is thought to be closer to the Sun than Sgr A\*), they find  $R_0 = 7.9^{+0.8}_{-0.7}$  kpc. Their associated measurement uncertainty, of order 10% for the first year's data, will further reduce with an increasing time baseline, as  $\sigma_{R_0} \propto 1/\sqrt{N}$  for N similar yearly observations.

OH/IR stars, of which many are found close to the Galactic Centre, can also potentially be used for determination of  $R_0$ . To do so would require direct measurements of both the angular diameter of the OH maser shell<sup>7</sup> using radio interferometry and the light travel time

 $<sup>^7</sup>$  SiO masers typically occur at radii of  $\sim$ 8 a.u. (astronomical units) for Mira variables, which corresponds to  $\sim$ 1 mas at  $R_0 \approx 8$  kpc.

across the shell, based on the time lag between red- and blueshifted emission from the shell's far and near sides, respectively (cf. Schultz *et al.* 1978; Jewell *et al.* 1980). However, VLBI observations have shown that the angular sizes of OH/IR shells near the Galactic Centre are strongly affected by scattering off electrons in the interstellar medium (van Langevelde and Diamond 1991; Frail *et al.* 1994; Lazio *et al.* 1999), hence preventing measurements of intrinsic shell sizes and, thus, a direct determination of  $R_0$ . The scattering scales with wavelength as  $\lambda^2$  (Lo *et al.* 1981), so that only the highest-frequency (> 20 GHz) masers are potentially suitable for precision astrometry.

OH/IR stars often also host 22 GHz H<sub>2</sub>O and/or 43 GHz (J = 1 - 0) silicon oxide (SiO) masers in their circumstellar shells (e.g. Habing 1996 and references therein). Although H<sub>2</sub>O masers are highly variable, SiO masers are more stable. The latter can, therefore, potentially be used for astrometry in the Galactic Centre region (e.g. Menten et al. 1997; Sjouwerman et al. 1998, 2002; Reid et al. 2003). However, relatively few SiO masers are known to be associated with OH/IR stars near the Galactic Centre (Lindqvist et al. 1991; Sjouwerman et al. 2002), which has triggered searches for 43 GHz masers in other types of mid-IR sources with colours typical of circumstellar envelopes and in blind surveys of the Galactic Centre (see Sjouwerman et al. 2004 for a review). SiO masers at 43 GHz or even at 86 GHz (J = 2 - 1) should be readily observable in the much more numerous Mira, long-period and semi-regular variables, as well as red supergiant stars (e.g. Habing 1996; Messineo et al. 2002, 2004; Sjouwerman et al. 2004; and references therein). This potentially offers an independent confirmation of distances determined based on periodluminosity analysis. The latter are also affected by numerous systematic uncertainties, such as an ambiguous extinction law, a bias for smaller values of R<sub>0</sub> because of preferential sampling of variable stars towards the near side of the bulge owing to extinction, and an uncertainty in characterizing how a mean distance to the group of variable stars relates to R<sub>0</sub> (cf. Gould et al. 2001; Udalski 2003; Ruffle et al. 2004; Kunder and Chaboyer 2008; Majaess 2010; see also Chapter 6).

Current best estimates of  $R_0$  using secondary distance indicators include  $8.24 \pm 0.08$  (statistical)  $\pm 0.42$  (systematic) kpc based on Mira variables (Matsunaga *et al.* 2009; but see Groenewegen and Blommaert 2005:  $R_0 = 8.8 \pm 0.4$  kpc),  $7.7 \pm 0.4$  kpc for RR Lyrae based on statistical-parallax solutions (Dambis 2010) versus  $8.1 \pm 0.6$  kpc using RR Lyrae observed as part of the Optical Gravitational Lensing Experiment (Majaess 2010),  $7.9 \pm 0.3$  kpc based on  $\delta$  **Scuti** stars (McNamara *et al.* 2000; see Section 3.5.6) and  $7.8 \pm 0.6$  kpc using Cepheids (Majaess *et al.* 2009). Vanhollebeke *et al.* (2009) considered both the full 3D stellar population mixture in the Galactic bulge, including its **metallicity** distribution, and the red clump stars alone, and concluded that  $R_0 = 8.7^{+0.57}_{-0.42}$  kpc. Their large distance disagrees, however, with the recent Babusiaux and Gilmore (2005) and Nishiyama *et al.* (2006) distance determinations based on near-IR data for the red clump (cf. Section 3.2.2).

#### 1.1.2.2 Orbital Modelling

Careful analysis of the stellar motions in the inner regions of the Milky Way can potentially result in a distance estimate to the Galactic Centre with significantly reduced uncertainties. Genzel *et al.* (2000) derived a primary distance (statistical parallax; see Section 2.1.3) of  $8.0 \pm 0.9$  kpc ( $1\sigma$ ) based on a statistical comparison of proper motions and line-of-sight velocities of stars in the central 0.5 pc, updated to  $R_0 = 7.2 \pm 0.9$  kpc by Eisenhauer *et al.* (2003) and subsequently to  $R_0 = 8.07 \pm 0.32 \pm 0.12$  kpc (statistical and systematic uncertainties, respectively) by Trippe *et al.* (2008). Diffraction-limited near-IR observations

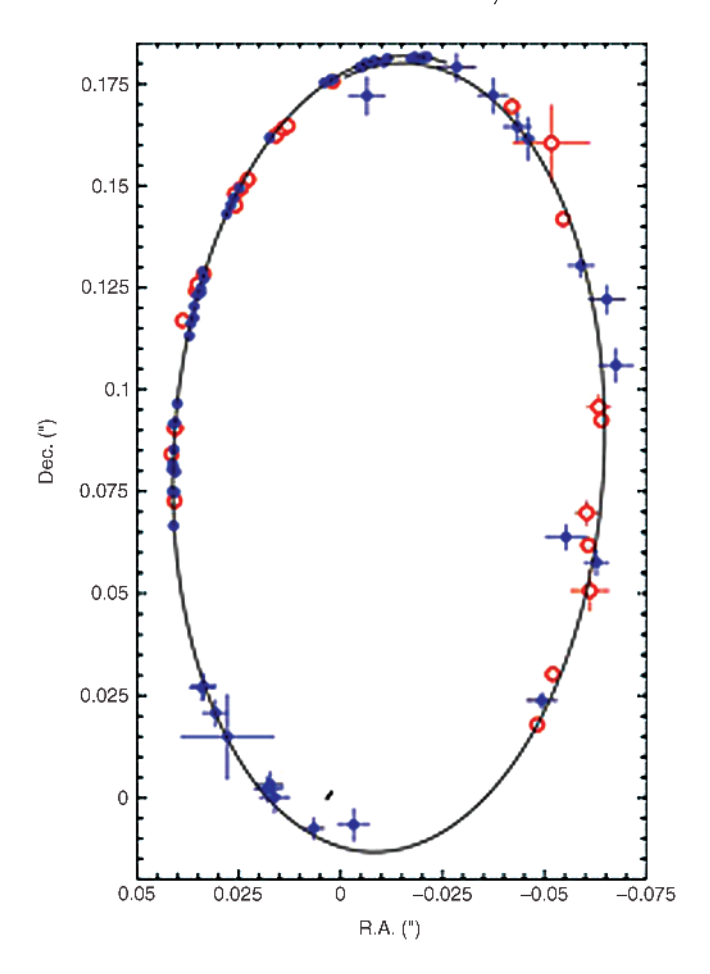


**Figure 1.6** Orbital fit for the Galactic Centre star S2 (Gillessen et al. 2009b). Blue: New Technology Telescope/Very Large Telescope (European Southern Observatory) measurements. Red: Keck telescope measurements. Black line: Keplerian fit. R.A., Dec.: right ascension, declination. (Reprinted from S. Gillessen, et al., Astrophysical Journal, **707**, The orbit of the star S2 around Sgr A\* from Very Large Telescope and Keck data, L114–L117, Copyright 2009, with permission of the AAS and S. Gillessen.)

of the Galactic Centre reveal  $\approx 100 \, \mathrm{S} \, \mathrm{stars}^8$  within 1" of Sgr A\*. The positions of the brightest sources can be measured to astrometric accuracies of 200–300  $\mu$ as (limited by crowding effects) using *K*-band adaptive-optics observations (Ghez *et al.* 2008; Fritz *et al.* 2010), while radial velocities with a precision of  $\sim 15 \, \mathrm{km \ s^{-1}}$  for the brightest early-type stars are typical (based on adaptive optics-assisted integral-field spectroscopy), decreasing to  $\sim 50-100 \, \mathrm{km \ s^{-1}}$  for fainter objects. The combined data set has enabled determination of

<sup>&</sup>lt;sup>8</sup> Eckart and Genzel (1996) identified the remarkably fast-moving stars in the 'Sgr A\* cluster' which were known at that time by 'S' followed by a number. The number of S stars has since grown to more than 200 (Ghez *et al.* 2008; Gillessen *et al.* 2009b; but note that both groups use different nomenclature).

the orbits of some 30 stars (Eisenhauer *et al.* 2003, 2005; Ghez *et al.* 2005, 2008; Gillessen *et al.* 2009b).

S2, the brightest of the S stars in the Galactic Centre, has completed a full revolution around Sgr A\* since high-resolution astrometric observations first became possible in 1992. It has an orbital period of 15.9 years and traces a highly elliptical Keplerian orbit with an orbital semi-major axis of 125 mas (see Figure 1.6; Schödel *et al.* 2002; Ghez *et al.* 2008; Gillessen *et al.* 2009a,b). Using a '**dynamical parallax**' approach (see Section 2.2) allows estimation of  $R_0$  (cf. Salim and Gould 1999), of which the accuracy is currently limited by systematic uncertainties:  $R_0 = 8.28 \pm 0.15$  (statistical)  $\pm 0.30$  (systematic) kpc (Gillessen *et al.* 2009a). This, in turn, constrains the black hole mass contained within its orbit to  $M_{\rm BH} = [4.30 \pm 0.06$  (statistical)  $\pm 0.35$  (due to uncertainties in  $R_0$ )]  $\times 10^6$  M $_{\odot}$ . A similar black hole mass of  $M_{\rm BH} = (4.5 \pm 0.4) \times 10^6$  M $_{\odot}$  was derived independently by Ghez *et al.* (2008), for  $R_0 = 8.4 \pm 0.4$  kpc (see also the review of Genzel *et al.* 2010).

In principle, to fully solve the equations governing two masses orbiting each other requires determination of six phase-space coordinates for each mass, as well as the two masses (e.g. Salim and Gould 1999). However, given the observational and systematic uncertainties, the mass of the star  $(m_{\rm S2}/m_{\rm Sgr~A^*}\sim 5\times 10^{-6})$  and the three velocity components of Sgr A\* can be neglected without accuracy penalties (Eisenhauer *et al.* 2003), provided that it is at rest with respect to the stellar cluster at the Galactic Centre. In addition, after subtraction of the motions of the Earth and the Sun around the Galactic Centre, the proper motion of Sgr A\* is  $-7.2\pm 8.5$  and  $-0.4\pm 0.9$  km s<sup>-1</sup> in the plane of the Milky Way in the direction of the rotation and towards the Galactic pole, respectively (Reid and Brunthaler 2004, with updates by Reid *et al.* 2009a; see also Backer and Sramek 1999; Reid *et al.* 1999, 2003), so that the velocity of Sgr A\* is <1% of that of S2. Thus, the current best estimate of the distance to the Galactic Centre has an associated combined uncertainty of  $\pm 0.34$  kpc.

#### 1.2 The Distance to the Large Magellanic Cloud

The Magellanic Clouds, and in particular the Large Magellanic Cloud, represent the first rung on the extragalactic distance ladder. The galaxy hosts statistically large samples of potential 'standard candles' (objects with the same absolute magnitude), including many types of variable stars. They are all conveniently located at roughly the same distance – although for detailed distance calibration the LMC's line-of-sight depth and 3D morphology must also be taken into account – and relatively unaffected by foreground extinction. The LMC's unique location allows us to compare and, thus, cross-correlate and calibrate a variety of largely independent distance indicators, which can, in turn, be applied to more distant targets. The distance to the LMC has played an important role in constraining the value of the Hubble constant, H<sub>0</sub>, the single most important parameter for determining the age and size of the Universe and (with CMB fluctuations) the amount of dark matter and the equation of state of dark energy, i.e. the ratio of the dark energy's pressure and density. The Hubble Space Telescope (HST) **Key Project** estimated  $H_0 = 72 \pm 3$  (statistical)  $\pm 7$ (systematic) km s<sup>-1</sup> Mpc<sup>-1</sup> (Freedman et al. 2001). Most notably, the  $\sim$ 10% systematic uncertainty is predominantly driven by the uncertainty in the assumed distance to the LMC (Reid et al. 2009b). Closer to home, proper-motion measurements of objects in the LMC are

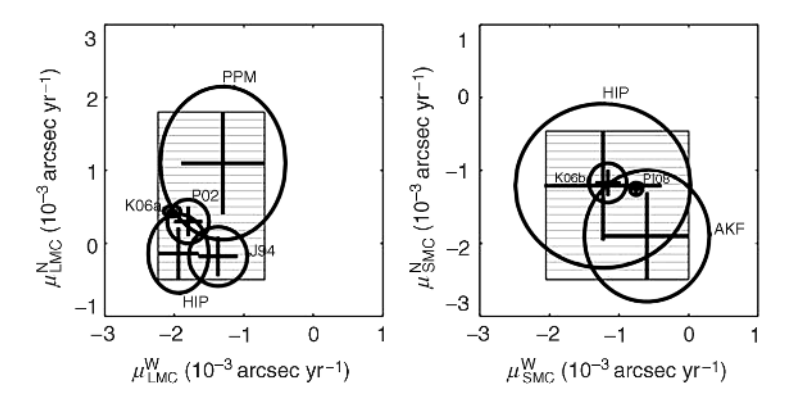


**Figure 1.7** Two-dimensional projections of the proper motions (North, West) for both the LMC and the SMC (Růžička et al. 2009). K06a,b: Kallivayalil et al. (2006a,b). Pl08: Piatek et al. (2008). J94: Jones et al. (1994). PPM: Kroupa et al. (1994). HIP: Kroupa and Bastian (1997). P02: Pedreros et al. (2002). AKF: combination of Freire et al. (2003) and Anderson and King (2004a,b). The ellipses show the 68.3% confidence regions. (Reprinted from A. Růžička et al., Astrophysical Journal, **691**, Spatial motion of the Magellanic Clouds: tidal models ruled out?, p. 1807–1815, Copyright 2009, with permission of the AAS and A. Růžička.)

now coming within reach (cf. Gardiner and Noguchi 1996; Kallivayalil *et al.* 2006a,b; Piatek *et al.* 2008; Costa *et al.* 2009), with major progress in this area expected from precision astrometric measurements in the *Gaia* era (see Section 2.1.2). A reliable distance estimate to the LMC is of crucial importance to assess future evolution scenarios of the Milky Way–LMC–Small Magellanic Cloud (SMC) system in the context of the Local Group of galaxies (e.g. Kallivayalil *et al.* 2006a,b, 2009; Besla *et al.* 2007; Bekki 2008; Růžička *et al.* 2009; and references therein; see also Figure 1.7).

It has become common practice to quote the distance to the LMC as a reddeningcorrected distance modulus,  $(m-M)_0$ . Most modern determinations cluster around  $(m-M)_0 = 18.5$  mag (e.g. Schaefer 2008; Szewczyk et al. 2008; and references therein). This was the value eventually settled on by the HST Key Project (Freedman et al. 2001; see also Section 4.1),  $(m - M)_0 = 18.50 \pm 0.10$  mag  $(50.1^{+1.4}_{-1.2} \text{ kpc})$ ; cf. Freedman and Madore 1991), and is currently considered the consensus distance modulus. Freedman et al. (2001) used a revised calibration of the Cepheid period-luminosity relation based on the maser-based distance to NGC 4258 (see Section 3.7.4) as well as several secondary distance measurement techniques - including Cepheids, RR Lyrae, Mira and eclipsing variables, the tip of the red giant branch (TRGB) as a standard candle, calibration of the red clump and supernova (SN) 1987A light echoes (see, respectively, Sections 3.5.2, 3.5.5, 3.5.3, 3.7.3, 3.3.1, 3.2.2 and 3.7.2) over the range from approximately 60 to 400 Mpc – to estimate the distance to the LMC. Many articles have focussed on obtaining a reliable distance to the LMC (see, for recent compilations, Westerlund 1997; Cole 1998; Gibson 2000; Freedman et al. 2001; Benedict et al. 2002; Clementini et al. 2003; Tammann et al. 2003; Walker 2003; Alves 2004; Schaefer 2008) using a range of methods, each of which has, in turn, been calibrated based on numerous independent techniques. For instance, calibration of the most often used Cepheid period-luminosity relation is commonly achieved using the surface brightness/Baade-Wesselink method, main-sequence fitting based on Galactic

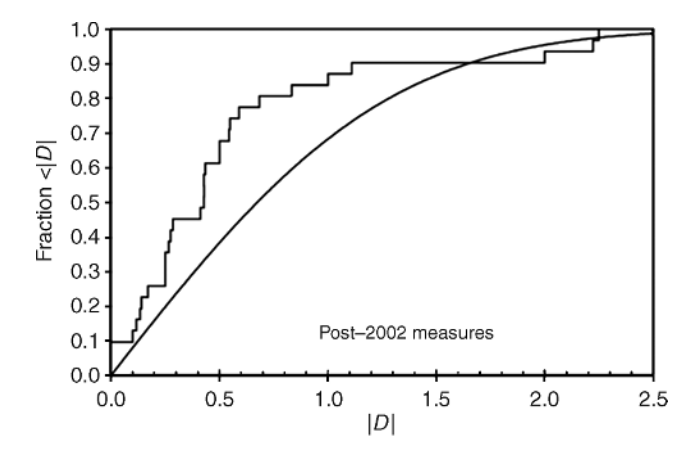


**Figure 1.8** Cumulative distributions of |D| from observations and for Gaussian errors (Schaefer 2008), where  $D = (\mu - 18.50)/\sigma$ ,  $\mu$  is the distance modulus and  $\sigma$  the observational uncertainty. The Kolmogorov–Smirnov test is a comparison between the cumulative distributions of |D| from observations (stepped curve) and the model (smooth curve). If the published values of the LMC distance modulus are unbiased and have correctly reported error bars, the two curves should lie relatively close together. If all but a few of the 31 post-2002 values included are too tightly clustered about the HST Key Project value of  $\mu = 18.50$  mag, the observed curve should step high above the model curve. The maximum deviation between the two curves is 0.33 at |D| = 0.59, which is very unlikely if the published data report unbiased values with correct error bars. (Reprinted from B. E. Schaefer, Astronomical Journal, 135, A problem with the clustering of recent measures of the distance to the Large Magellanic Cloud, p. 112–119, Copyright 2008, with permission of the AAS and B. E. Schaefer.)

open cluster and/or GC colour–magnitude diagrams, nonlinear pulsation modelling, and *Hipparcos* and *HST* parallaxes (see, respectively, Sections 3.5.1, 3.2.1, 3.5.5 and 2.1.2).

Although the published LMC distance moduli before Freedman *et al.*'s 2001 article covered the range from ~18.1 to 18.8 mag, corresponding to distances from 42 to 58 kpc, <sup>9</sup> with much smaller individual error bars than the overall spread of the values, the wide scatter suddenly disappeared after the results of the *HST* Key Project were published, with a 'true' distance modulus of  $18.50 \pm 0.02$  mag implied by the 14 measurements published between 2001 and 2004 (Alves 2004; see also Schaefer 2008). Schaefer (2008) notes that this situation, in which most methods were originally dominated by large, mostly unrecognized systematic errors, which then essentially disappeared overnight, is disturbing. (The same is not seen for the smaller number of distance determinations to the SMC, which might imply that the LMC effect is caused by 'sociological' or 'bandwagon' behaviour, also known as 'publication bias'. The SMC was not included in the *HST* Key Project.) He argues that all  $14 (m - M)_0$  values published between 2001 and 2004 are *too* consistent with the *HST* Key Project's result:  $(m - M)_0 = 18.50$  mag falls within the  $1\sigma$  uncertainty for all 14 determinations, corresponding to an improbably low  $\chi^2$  statistical probability of 0.0022 (Schaefer 2008; see Figure 1.8).

<sup>&</sup>lt;sup>9</sup> Historically, there has been vigorous debate supporting a 'long' versus 'short' distance modulus: see Fouqué et al. (2007) and Sandage et al. (2009) for recent results in favour of the 'short' distance scale, often resulting from application of statistical parallaxes and the Baade–Wesselink method (see also de Vaucouleurs 1993a,b; Gratton et al. 1997; Clementini et al. 2003). However, this has largely disappeared after publication of Freedman et al. (2001).

In fact, Schaefer (2008) further extended his analysis of LMC distance moduli published after 2002 – including a total of 31 independent measurements, without substantial overlap of targets or correlations between publications – and concluded that there is a clear statistical overabundance of determinations that agree with the HST Key Project to much greater accuracy than the quoted error bars: a Kolmogorov-Smirnov test (a nonparametric test that allows statistical comparison of two one-dimensional distributions; Press et al. 1992) proves that the distribution of the published distance moduli deviates from the expected Gaussian profile at the  $>3\sigma$  level. This calls into serious doubt the reliability of LMC distance moduli determined since 2002, because there are only two ways in which such a statistical condition can be met, either by artificially adjusting or selecting the published values to be near  $(m-M)_0 = 18.50$  mag or by systematically overestimating the error bars (which is unlikely; Schaefer 2008). Clearly, this is a very unfortunate situation, given that the distance to the LMC is a crucial step towards the calibration of extragalactic distances! To remedy this situation, a comprehensive and independent recalibration, including realistic error bars, of the current best data set of reliable distance indicators seems unavoidable. Alternatively, new maser- or eclipsing binary-based direct methods of distance determination may provide an independent means of calibrating the first rung of the extragalactic distance ladder (cf. Herrnstein et al. 1999; Macri et al. 2006; Di Benedetto 2008; Pietrzyński et al. 2009; see also Sections 3.7.4, and 1.3 and 3.7.3, respectively).

An interesting alternative is offered by the coming online of large-scale near-IR survey capabilities with access to the Magellanic Clouds, which will essentially eliminate the effects of reddening and provide an independent and highly reliable calibration approach (e.g. Nemec *et al.* 1994; Bono 2003; Szewczyk *et al.* 2008; and references therein). Although efforts are continuing to further refine the LMC distance based on near-IR observations (see Table 1.1 for an update since Schaefer 2008), large-scale surveys such as the *VISTA* near-IR

Table 1 1	Published LMO	distance de	aterminations	cinco	Schapfor (200	101
labie L.i	PHOUSINED LIVI	$-\alpha$	-10111111111111111111111111111111111111		Maeier (700)	$I \cap I$

Date	Article	$(m-M)_0$ (mag)	(Opt./NIR) Method
Aug. 2007	van Leeuwen <i>et al</i> .	$18.39 \pm 0.05$	(Opt.) Cepheids
Jan. 2008	Clement et al.	$18.49 \pm 0.11$	(Opt.) RR Lyrae
Mar. 2008	Sollima et al.	$18.56 \pm 0.13$	(NİR) RR Lyrae <sup>a</sup>
Apr. 2008	Catelan and Cortés	$18.44 \pm 0.11$	(Opt.) RR Lyrae
Jun. 2008	Ngeow and Kanbur	$18.48 \pm 0.03$	(NIR) Cepheids <sup>b</sup>
		$18.49 \pm 0.04$	(NIR) Cepheids <sup>b</sup>
Jul. 2008	Szewczyk et al.	$18.58 \pm 0.03$ (stat.)	(NIR) RR Lyrae
	·	$\pm 0.11$ (syst.)	·
Nov. 2008	Di Benedetto	$18.559 \pm 0.003$ (stat.)	(Opt.) Cepheids
		$\pm 0.026$ (syst.)	
May 2009	Pietrzyński <i>et al</i> .	$18.50 \pm 0.55$	Eclipsing binary
Jun. 2009	Dambis	$18.27 \pm 0.08$	(NIR) RR Lyrae
Jul. 2009	Koerwer	$18.54 \pm 0.06$	(NIR) Red clump
Aug. 2009	Borissova et al.	$18.53 \pm 0.13$	(NIR) RR Lyrae
		$18.46 \pm 0.07$	(NIR) Red clump
Aug. 2009	Matsunaga et al.	$18.46 \pm 0.10$	(NIR) Cepheids
Jun. 2010	Reid and Parker	$18.46 \pm 0.2$	Planetary nebulae

<sup>&</sup>lt;sup>a</sup> To Reticulum.

<sup>&</sup>lt;sup>b</sup> Using a linear and a broken period-luminosity relation, respectively.

 $YJK_s$  survey of the Magellanic system (Cioni *et al.* 2008, 2011) hold the promise of finally reducing the systematic uncertainties and settling the distance to the LMC conclusively, with remaining uncertainties in the distance modulus of  $\ll 0.1$  mag.

## 1.3 Benchmarks Beyond the Magellanic Clouds: the 3D Universe on Large(r) Scales

Beyond the Magellanic Clouds, the next logical object for distance benchmarking is the Andromeda galaxy (M31), the other large spiral galaxy – in addition to the Milky Way – in the Local Group<sup>10</sup> (see also Brunthaler et al. 2005 for a case in favour of M33 as distance anchor, although see footnote 11). Once its distance is known to sufficient accuracy, all of its various stellar populations are available as potential standard candles. M31 is a potentially crucial rung on the extragalactic distance ladder (Clementini et al. 2001; Vilardell et al. 2006, 2010). First, its distance is sufficiently large,  $744 \pm 33$  kpc or  $(m - M)_0 = 24.36 \pm 0.08$ mag (Vilardell et al. 2010: direct estimate based on two eclipsing binary systems), that poorly constrained geometry effects do not cause additional significant systematic uncertainties, as for the Magellanic Clouds. Second, individual stars suitable for calibration of extragalactic distances (Cepheid or RR Lyrae variables, eclipsing binaries, novae and SNe, as well as GCs, for instance) can be observed fairly easily and are affected by only moderate extinction and reddening, with a **colour excess**  $E(B-V) \equiv A_B - A_V = 0.16 \pm 0.01$  mag (Massey et al. 1995). Finally, as a mid-type spiral galaxy, it has a chemical composition and morphology similar to that of the Milky Way and other galaxies commonly used for distance determination (e.g. Freedman et al. 2001) and it can be used for absolute local calibration of the Tully-Fisher relation, one of the commonly used distance indicators to more distant spiral galaxies (see Section 4.5).

The compilation of published distance estimates of Vilardell et al. (2006) shows that most methods return best estimates between  $(m-M)_0 = 24.0$  and 24.5 mag, with the majority of recent measurements tending towards the greater-distance end of this range. For instance, Holland (1998), Stanek and Garnavich (1998), Durrell et al. (2001), Joshi et al. (2003, 2010), Brown et al. (2004), McConnachie et al. (2005), Clementini et al. (2009) and Sarajedini et al. (2009) all reported  $(m - M)_0 \in [24.46, 24.52]$  mag – based on analysis of tracers as diverse as the red giant branch (Section 3.3, particularly Section 3.3.2), red clump (Section 3.2.2), Cepheids (Section 3.5.2), RR Lyrae (Section 3.5.5) and the TRGB (Section 3.3.1) – with uncertainties of generally  $\Delta(m-M)_0 < 0.10$  mag, although the type I and II Cepheid-based distances reported by Vilardell et al. (2007) and Majaess et al. (2010) are somewhat shorter. This situation is reminiscent of that of the LMC, in the sense that the distribution is narrower than the expected Gaussian profile. Hence, exercise of caution is needed. The direct, eclipsing binary-based distance determinations to M31 (Ribas et al. 2005; Vilardell et al. 2010; see also Bonanos et al. 2003) agree very well with independent Cepheid distances (e.g. Vilardell et al. 2007; see also Vilardell et al. 2006, their Table 1). In turn, these are based on either an eclipsing binary calibration of the LMC

<sup>&</sup>lt;sup>10</sup> The Local Group is a loose galaxy association with a core radius of order 1 Mpc centred on the Milky Way–M31 barycentre. Its member galaxies are characterized by velocities which are close to the velocity–position relations satisfied by most known Local Group members.

distance (e.g. Fitzpatrick *et al.* 2003) or a maser-based distance determination to NGC 4258 (Macri *et al.* 2006). <sup>11</sup> The latter object has been suggested as an alternative yet highly robust benchmark for anchoring of the local distance calibration (Riess *et al.* 2009a). Prospects of 1% level *direct, geometric* distance determinations to M31 and M33 look promising, e.g. by employing time-delayed, dust-scattered X-ray haloes (Section 7.3; see for application to M31, Draine and Bond 2004) or – with significantly improved astrometric precision (see Section 2.1.2) – using novel '**rotational parallax**' measurements (Peterson and Shao 1997; Olling and Peterson 2000; Brunthaler *et al.* 2005; Olling 2007) combined with galactic velocity fields (see also Gould 2000) and, thus, improved distance precision (cf. Shaya and Olling 2009). The latter are the extragalactic equivalent to the 'orbital parallax' method for resolved binary systems, where radial velocities and proper motions of visual binaries are combined to derive the orbital parameters as well as the distance (e.g. Armstrong *et al.* 1992; Davis *et al.* 2005).

The importance of accurate distance determinations cannot be overstated. Despite significant efforts and worldwide coordination, even for the nearest objects the field is not free from controversy. For instance, the long-standing distance determination to the Orion Nebula – in particular to the high-mass star-forming Becklin–Neugebauer/Kleinmann–Low (KL) region – of  $480 \pm 80$  pc (Genzel et al. 1981), which was based on VLBI observations of 22 GHz H<sub>2</sub>O maser features, was recently significantly revised to  $d = 389^{+24}_{-21}$  pc (see Figure 1.9; Sandstrom et al. 2007; and review of previous determinations therein). Sandstrom et al. (2007) employed 15 GHz VLBA radio-continuum observations, which yielded the parallax (see also Bertout et al. 1999 for Hipparcos-based results) and proper motion of the flaring, nonthermal radio star GMR A in the Orion Nebula Cluster (see also Hirota et al. 2007; Jeffries 2007; Kraus et al. 2007). Similarly, Menten et al. (2007) used VLBA radio-continuum observations at 8.4 GHz to determine a trigonometric parallax of several member stars of the Orion Nebula Cluster which exhibited nonthermal radio emission. They concluded that  $d=414\pm7$  pc, in agreement with the results of both Kraus et al. (2007) and Kim et al. (2008). The latter were based on orbital solution modelling of the  $\theta^1$  Orionis C close binary system and parallactic SiO maser observations of the Orion-KL region using VLBI, respectively. These more modern parallactic determinations are fully model independent, as opposed to Genzel et al. 's measurement, which required assumptions about the distribution of the masers and application of an expanding, thick-shell model. A 10% shorter distance than previously adopted results in 10% lower masses, 20% fainter luminosities and 20–30% younger ages for the stars in the Orion Nebula region.

Accurate distances are clearly also important to determine the physical properties of the stars, star clusters, peculiar objects (such as ultraluminous X-ray sources) and gas clouds in galaxies beyond the Local Group, and to assess their structure and internal as well as external dynamics (for the latter, see e.g. de Grijs and Robertson 2006). The recent controversy surrounding the Antennae interacting galaxies (NGC 4038/4039) provides an illustrative example. New *HST* observations of the TRGB in this system seemed to imply a significantly shorter distance (from  $d \sim 20$  to  $13.3 \pm 1.0$  Mpc; Saviane *et al.* 2008) than previously adopted based on a careful assessment of the system's

<sup>&</sup>lt;sup>11</sup> For the third largest Local Group galaxy M33, the Triangulum galaxy, a systematic discrepancy remains between the eclipsing binary distance of Bonanos *et al.* (2006), the Cepheid determination of Freedman *et al.* (2001) and the maser-based distance of Brunthaler *et al.* (2005), in the sense that the eclipsing binary determination places the galaxy 0.3 mag more distant than the other methods.

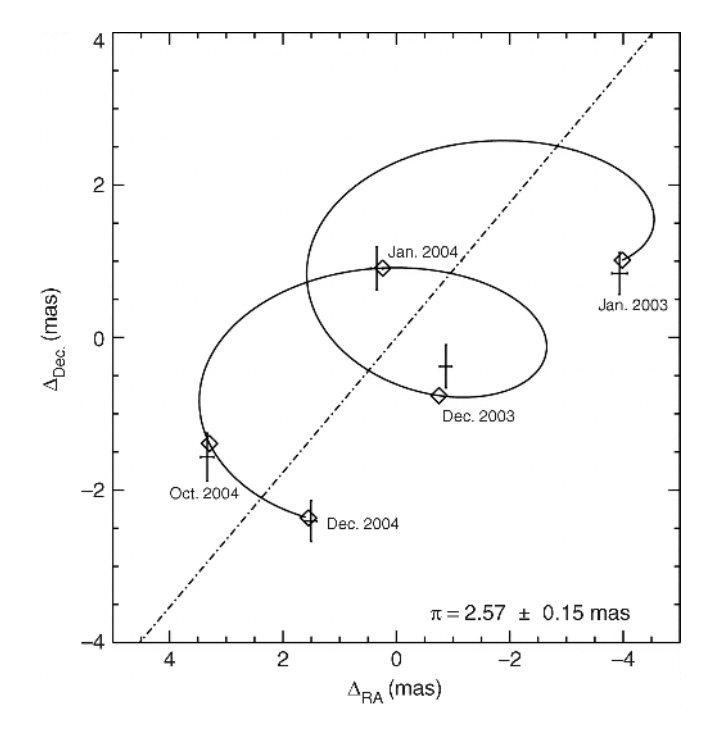


**Figure 1.9** Measured positions (diamonds) of the flaring, nonthermal radio star GMR A in the Orion Nebula Cluster with the best-fitting parallax and proper motion (Sandstrom et al. 2007). The dot-dashed line is the proper motion of the source, with the parallactic motion subtracted. The trigonometric parallax ( $\pi$ ) corresponds to a distance of  $389^{+24}_{-21}$  pc. (Reprinted from K. M. Sandstrom et al., Astrophysical Journal, **667**, A parallactic distance of 389 parsecs to the Orion Nebula Cluster from Very Long Baseline Array observations, p. 1161–1169, Copyright 2007, with permission of the AAS and K. M. Sandstrom.)

recession velocity, adoption of a reasonable value for  $H_0$  and including proper corrections for the local **Hubble flow** (see Section 5.1). However, Schweizer *et al.* (2008) pointed out that not only would the Antennae system's size, mass and luminosity – as well as the equivalent properties of the galaxies' constituents – reduce, but its heliocentric velocity would also deviate by close to  $3\sigma$  from the best large-scale flow model were this shorter distance adopted (see Figure 1.10). Using observations of the Type Ia SN 2007sr, an excellent standard candle<sup>12</sup> (see Section 5.2.1), they derive an independent distance estimate to the interacting system of  $d = 22.3 \pm 2.8$  kpc. They suggest that Saviane *et al.*'s (2008) shorter distance determination may have had its origin in a misidentification of the TRGB. Schweizer *et al.* report a preliminary  $d_{TRGB} = 20.0 \pm 1.6$  Mpc, based on a reanalysis of the same *HST* data.

Beyond the nearest, well-resolved galaxies, the tool of choice for distance determinations has traditionally been the use of galaxies' recessional velocities and, hence, redshifts.

 $<sup>^{12}</sup>$  If Saviane *et al.*'s (2008) distance were correct, SN 2007sr's peak luminosity would differ by  $\sim 7\sigma$  (or 1.1 mag) from the mean peak luminosity of SNe Ia.

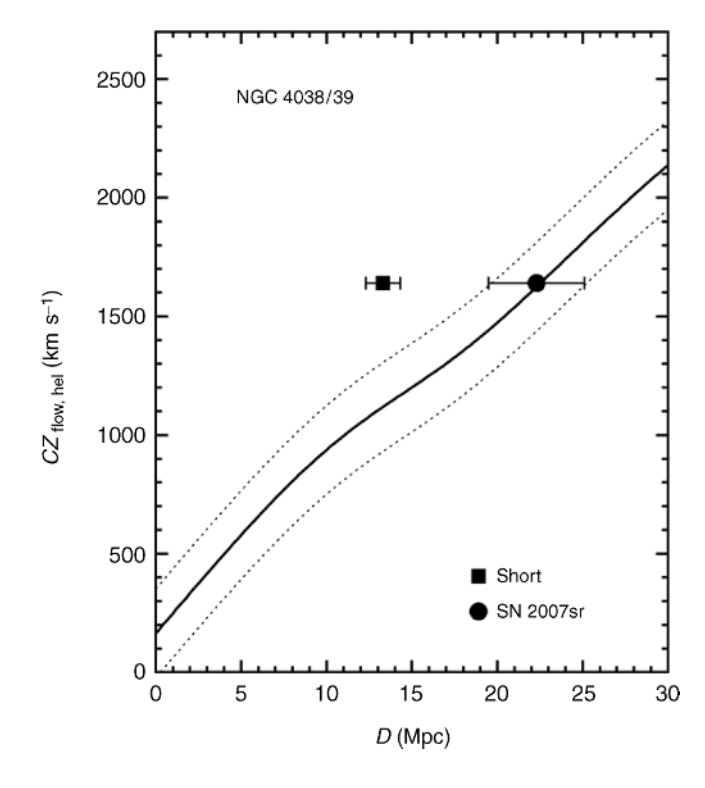


**Figure 1.10** Comparison of distances (D) measured for NGC 4038/39 (points) with a relevant large-scale flow model (solid line).  $cz_{hel}$ : heliocentric recession velocity. Plotted at the new distance based on Type Ia SN 2007sr (filled dot), the recession velocity of NGC 4038/39 falls well within  $1\sigma_{th}$  (dotted lines) of the large-scale flow, where  $\sigma_{th}$  is the cosmic random radial velocity. In contrast, when plotted at the short distance based on the TRGB (square, Saviane et al. 2008), the recession velocity of NGC 4038/39 lies 522 km s<sup>-1</sup> or 2.8 $\sigma$  above the flow (Schweizer et al. 2008). (Reprinted from F. Schweizer et al., Astronomical Journal, **136**, A new distance to the Antennae galaxies (NGC 4038/39) based on the Type Ia supernova 2007sr, p. 1482–1489, Copyright 2008, with permission of the AAS and F. Schweizer.)

Although this technique works reasonably well in the smooth Hubble flow (see Section 5.1.2), the mutual attractive forces of galaxies within the gravitational potential wells of large galaxy clusters cause significant 'peculiar motions' and, hence, distort the distance-redshift relationship. Observationally, this results in an elongation of the positions, in redshift space, of galaxy cluster members along the line of sight, which is commonly referred to as the 'Finger-of-God' effect (see also Section 5.1.2).

In recent years, distance measurements to significant numbers of nearby cluster galaxies have become available, thus allowing studies of the true 3D distributions of the Virgo and Fornax clusters. This has led to the realization that the Virgo cluster is, in fact, highly substructured (e.g. West and Blakeslee 2000; Solanes *et al.* 2002; Jerjen 2003; Mei *et al.* 2005, 2007). Using the technique of **surface brightness fluctuations** (SBFs; see Section 4.2), West and Blakeslee (2000) and Jerjen *et al.* (2004) revealed strong 3D substructure and bimodality along the line of sight in the cluster's northern regions. The latter authors

concluded that the northern subcluster consists of two dynamically distinct systems, with a small group around M86 falling into the M87 subcluster from behind.

Based on their detailed analysis of the SBFs in the statistically homogeneous and significant samples of Virgo and Fornax cluster galaxies, Mei et al. (2005, 2007) and Blakeslee et al. (2009, 2010) recently provided new and much improved insights into the 3D distribution of these clusters' member galaxies. Blakeslee et al. (2009) find a very tight correlation between the mean  $z_{850}$  magnitudes and  $(g_{475} - z_{850})$  colours (where the subscripts in the filter names denote their central wavelengths in nanometres) of early-type galaxies in the Fornax cluster ( $d = 20.0 \pm 0.2 \pm 1.4$  Mpc, where the errors are statistical and systematic, respectively), which allows these authors to obtain a first estimate of the 'cosmic' scatter in the relation, i.e. the scatter caused by the cluster's depth,  $\sigma_{\cos} \approx 0.06 \pm 0.01$  mag, assuming a 20% depth uncertainty. This estimated scatter is approximately 40% smaller than that for the Virgo cluster (Mei et al. 2005, 2007; after correction of the latter depth estimates by a factor  $1/\sqrt{2}$ , which was omitted by these authors; see also Tonry et al. 2000), which implies that the former is more compact along the line of sight and exhibits less substructure (see e.g. Dunn and Jerjen 2006 and references therein). Blakeslee et al. (2009) derive a true linear root-mean-square depth for the bright ( $B_T \le 15.5$  mag), early-type galaxies in the Fornax cluster of  $\sigma_d = 0.49^{+0.11}_{-0.15}$  Mpc, implying a back-to-front  $\pm 2\sigma_d$  distance depth of  $2.0^{+0.4}_{-0.6}$ Mpc (see Figure 1.11). This is comparable to the earlier, independent depth estimate of

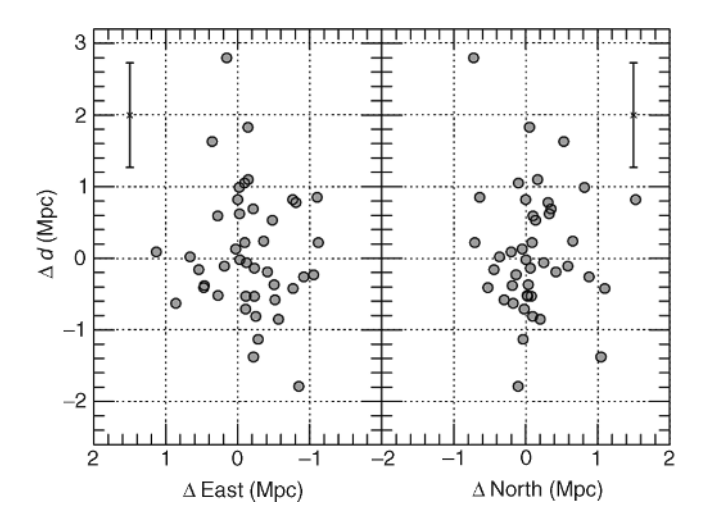


**Figure 1.11** Galaxy distance in the Fornax cluster, with respect to the mean distance of 20 Mpc, versus physical offset in Mpc east—west (left panel) and north—south (right panel) with respect to the central, giant elliptical galaxy NGC 1399 (Blakeslee et al. 2009). The median error in  $\Delta d$  is shown in both panels. There is a bias towards the cluster appearing elongated along the line of sight caused by distance errors and because galaxies more than about 1.5 Mpc from the cluster mean would not be included in the underlying catalogue if the offset were in the plane of the sky rather than along the line of sight. (Reprinted from J. Blakeslee et al., Astrophysical Journal, **694**, The ACS Fornax Cluster Survey. V. Measurement and recalibration of surface brightness fluctuations and a precise value of the Fornax—Virgo relative distance, p. 556–572, Copyright 2009, with permission of the AAS and J. Blakeslee.)

the Fornax cluster core by Dunn and Jerjen (2006),  $\sigma_{\text{int}} = 0.74^{+0.52}_{-0.74}$  Mpc, which in turn is similar to the projected cluster size on the sky.

The prospects are promising for application of SBF approaches, based on high-resolution observations with the HST or large ground-based observatories, to galaxies in the Coma cluster, at  $d \sim 100$  Mpc (cf. Liu and Graham 2001). However, the choice of suitable distance tracers on these scales is limited. Here, well into the smooth Hubble flow, we must predominantly rely on bright standard candles for reliable distances, including Type Ia SNe (see Section 5.2.1). Although we do not yet fully understand the physics governing SNe Ia explosions, the relationship between their absolute magnitude at peak brightness, their colour and their rate of decline is among the tightest empirical tools available for distance determinations at moderate redshifts. It allowed Riess et al. (1998) and Perlmutter et al. (1999) to conclude independently that SNe Ia at  $z \sim 0.5$  appear to be approximately 10% fainter than their local counterparts. On the assumption that they were dealing with the same type of objects, they postulated that this implied that the expansion rate of the Universe is accelerating (see Figure 5.3; see, for reviews, Filippenko 2005; Frieman et al. 2008). From a physical perspective, this implies that the Universe must be subject to a large negative pressure, which has since been associated with Einstein's cosmological constant  $\Lambda$  and a vacuum energy denoted by  $\Omega_{\Lambda}$ , which has been coined 'dark energy'.

Beyond the redshifts currently accessible with best-established, fairly 'local' distance tracers, cosmologists are particularly interested in reducing the uncertainties in and precisely establishing the main cosmological parameters that determine the evolution of the Universe on the largest scales. The latter include, of course, the Hubble constant, but also the matter–energy density ( $\Omega_{\rm M}$ ), the curvature of the Universe – represented by the constant k, where k < 0, k = 0 and k > 0 corresponds to an open, flat and closed Universe – the dark energy's equation-of-state parameter (w) and  $\sigma_{8}$ , which measures the amplitude of the linear power spectrum on the scale of  $8h^{-1}$  Mpc, where h denotes the value of the Hubble constant in units of  $100 \text{ km s}^{-1}$  Mpc<sup>-1</sup>. In the context of this chapter and with the aim of achieving improved distance determinations, of these the current value of the Hubble constant is of greatest relevance (for a discussion of the prevailing cosmological model, see Section 5.1.3).

Significant strides have been made towards the goal of establishing the value of  $H_0$  with an accuracy of better than 10%. Locally, two independent teams have endeavoured to achieve this aim using a variety of well-established distance anchors (Freedman *et al.* 2001; Sandage *et al.* 2006), although the resulting values of  $H_0$  differ systematically: the *HST* Key Project (Freedman *et al.* 2001) derived a statistically weighted value of  $H_0 = 72 \pm 8 \text{ km s}^{-1}$  Mpc<sup>-1</sup>, while Sandage *et al.* (2006) found  $H_0 = 62.3 \pm 1.3$  (statistical)  $\pm 5.0$  (systematic) km s<sup>-1</sup> Mpc<sup>-1</sup>, an unsatisfactory outcome that remains an issue of contention (but see Riess *et al.* 2009a,b; see also Chapter 6).

Much progress has been achieved in the last few years. In particular, the 7-year results of the *Wilkinson Microwave Anisotropy Probe (WMAP)* (e.g. Komatsu *et al.* 2009, 2011 and references therein) have reduced the uncertainties in the large-scale Hubble constant to unprecedentedly low levels,  $H_0 = 70.4 \pm 2.5 \text{ km s}^{-1} \text{ Mpc}^{-1}$ . However, *WMAP* results rely on many different '**priors**' (pre-imposed constraints) and do not allow an independent determination of the Hubble constant. This is because the value of  $H_0$  is degenerate with the total curvature of the Universe. For instance, decreasing  $H_0$  by 20 km s<sup>-1</sup> Mpc<sup>-1</sup> reduces the total matter–energy density in the Universe by 0.1 in terms of  $\Omega_{\rm M}$ . In particular, the *WMAP*-supported value of  $H_0$  relies on the assumption of a flat geometry. When that

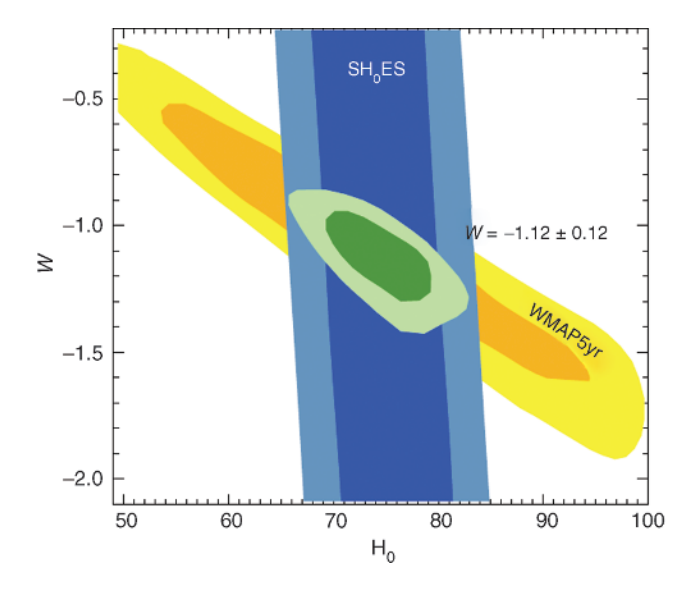


**Figure 1.12** Confidence regions in the plane of  $H_0$  and the dark energy's equation of state, w (Riess et al. 2009a). The localization of the third acoustic peak in the WMAP 5-year data (Komatsu et al. 2009) produces a confidence region which is narrow but highly degenerate in this space. The best constraints on the Hubble constant are  $H_0 = 74.2 \pm 3.6$  km s<sup>-1</sup> Mpc<sup>-1</sup>, while  $w = 1.12 \pm 0.12$  for a constant equation of state. This result is comparable in precision to determinations of w from baryon acoustic oscillations and high-redshift SNe Ia, but is independent of both. The inner and outer regions represent 68 and 95% confidence, respectively.  $SH_0ES$ : supernovae and  $H_0$  for the equation of state. (Reprinted from A. Riess et al., Astrophysical Journal, 699, A redetermination of the Hubble constant with the Hubble Space Telescope from a differential distance ladder, p. 539–563, Copyright 2009, with permission of the AAS and A. Riess.)

constraint is relaxed, the fitted value moves to  $H_0 = 53^{+15}_{-13} \, \mathrm{km \, s^{-1} \, Mpc^{-1}}$ : the central value has changed considerably, and the precision is much reduced.

Because of the dominant degeneracies precluding the direct and unambiguous determination of the value of the Hubble constant, cosmologists must rely on combining constraints resulting from many different approaches and tracers (see Section 5.3.4). For instance, the 5-year *WMAP* observations in combination with both SNe Ia and constraints from **baryon acoustic oscillations** (see Section 5.3.3) result in  $H_0 = 70.5 \pm 1.3$  km s<sup>-1</sup> Mpc<sup>-1</sup> (Komatsu *et al.* 2009), while combining observational redshift distributions of galaxies with constraints on the baryon and CDM densities from *WMAP-5* and SNe Ia, assuming essentially a flat geometry, yields  $H_0 = 68 \pm 2$  km s<sup>-1</sup> Mpc<sup>-1</sup> (Freedman and Madore 2010). Figure 1.12 shows an example of such an approach, in which the value of  $H_0$  is constrained based on a combination of *WMAP-5* data and observations of SNe Ia. Although the Hubble constant is currently known to better than 5%, provided that all priors and assumptions on a flat Universe hold, further improvements are urgently required to better constrain the nature of the elusive dark energy (cf. Riess *et al.* 2009a; see also Section 5.3.4).

#### **Bibliography**

- Alves DR 2004 A review of the distance and structure of the Large Magellanic Cloud. *New Astron. Rev.* **48**, 659–665.
- Anderson J and King IR 2004a Multi-filter PSFs and distortion corrections for the HRC. ACS Instrument Science Report 2004-15, 51 pp.
- Anderson J and King IR 2004b Erratum: The rotation of the globular cluster 47 Tucanae in the plane of the sky. *Astron. J.* **128**, 950–950.
- Armstrong JT, Mozurkewich D, Vivekanand M, Simon RS, Denison CS, Johnston KJ, Pan X-P, Shao M and Colavita MM 1992 The orbit of α Equulei measured with long-baseline optical interferometry: component masses, spectral types, and evolutionary state. *Astron. J.* **104**, 241–252.
- Babusiaux C and Gilmore G 2005 The structure of the Galactic bar. *Mon. Not. R. Astron. Soc.* **358**, 1309–1319.
- Backer DC and Sramek RA 1999 Proper motion of the compact, nonthermal radio source in the Galactic Center, Sagittarius A\*. *Astrophys. J.* **524**, 805–815.
- Bekki K 2008 A possible common halo of the Magellanic Clouds. Astrophys. J. 684, L87-L90.
- Belloche A, Menten KM, Comito C, Müller HSP, Schilke P, Ott J, Thorwirth S and Hieret C 2008 Detection of amino acetonitrile in Sgr B2(N). *Astron. Astrophys.* **482**, 179–196.
- Benedict GF, McArthur BE, Fredrick LW, Harrison TE, Lee J, Slesnick CL, Rhee J, Patterson RJ, Nelan E, Jefferys WH, van Altena W, Shelus PJ, Franz OG, Wasserman LH, Hemenway PD, Duncombe RL, Story D, Whipple AL and Bradley AJ 2002 Astrometry with the Hubble Space Telescope: a parallax of the fundamental distance calibrator RR Lyrae. *Astron. J.* 123, 473–484.
- Bertout C, Robichon N and Arenou F 1999 Revisiting Hipparcos data for pre-main sequence stars. *Astron. Astrophys.* **352**, 574–586.
- Besla G, Kallivayalil N, Hernquist L, Robertson B, Cox TJ, van der Marel RP and Alcock C 2007 Are the Magellanic Clouds on their first passage about the Milky Way? *Astrophys. J.* **668**, 949–967.
- Blakeslee JP, Jordán A, Mei S, Côté P, Ferrarese L, Infante L, Peng EW, Tonry JL and West MJ 2009 The ACS Fornax cluster survey. V. Measurement and recalibration of surface brightness fluctuations and a precise value of the Fornax–Virgo relative distance. *Astrophys. J.* **694**, 556–572.
- Bonanos AZ, Stanek KZ, Sasselov DD, Mochejska BJ, Macri LM and Kałużny J 2003 DIRECT distances to nearby galaxies using detached eclipsing binaries and Cepheids. IX. Variables in the field M31Y discovered with image subtraction. *Astron. J.* **126**, 175–186.
- Bonanos AZ, Stanek KZ, Kudritzki R-P, Macri LM, Sasselov DD, Kałużny J, Stetson PB, Bersier D, Bresolin F, Matheson T, Mochejska BJ, Przybilla N, Szentgyorgyi AH, Tonry J and Torres G 2006 The first DIRECT distance determination to a detached eclipsing binary in M33. *Astrophys. J.* **652**, 313–322.
- Bono G 2003 RR Lyrae distance scale: theory and observations. In *Proc. Stellar Candles for the Extragalactic Distance Scale* (eds Alloin D and Gieren W), *Lect. Notes Phys.* **635**, 85–104.
- Borissova J, Rejkuba M, Minniti D, Catelan M and Ivanov VD 2009 Properties of RR Lyrae stars in the inner regions of the Large Magellanic Cloud. III. Near-infrared study. *Astron. Astrophys.* **502**, 505–514.
- Brown TM, Ferguson HC, Smith E, Kimble RA, Sweigart AV, Renzini A and Rich RM 2004 RR Lyrae stars in the Andromeda halo from deep imaging with the Advanced Camera for Surveys. *Astron. J.* **127**, 2738–2752.
- Brunthaler A, Reid MJ, Falcke H, Greenhill LJ and Henkel C 2005 The geometric distance and proper motion of the Triangulum galaxy (M33). *Science* **307**, 1440–1443.
- Catelan M and Cortés C 2008 Evidence for an overluminosity of the variable star RR Lyrae, and a revised distance to the LMC. *Astrophys. J.* **676**, L135–L138.
- Cioni M-RL, Bekki K, Clementini G, de Blok WJG, Emerson JP, Evans CJ, de Grijs R, Gibson BK, Girardi L, Groenewegen MAT, Ivanov VD, Leisy P, Marconi M, Mastropietro C, Moore B, Naylor T, Oliveira JM, Ripepi V, van Loon JT, Wilkinson MI and Wood PR 2008 The Magellanic Clouds as a template for the study of stellar populations and galaxy interactions. *Publ. Astron. Soc. Aust.* **25**, 121–128.

- Cioni M-RL, Clementini G, Girardi L, Guandalini R, Gullieuszik M, Miszalski B, Moretti M-I, Ripepi V, Rubele S, Bagheri G, Bekki K, Cross N, de Blok WJG, de Grijs R, Emerson JP, Evans CJ, Gonzales-Solares E, Groenewegen MAT, Irwin M, Ivanov VD, Kerber L, Lewis J, Marconi M, Marquette J-B, Mastropietro C, Moore B, Napiwotzki R, Naylor T, Oliveira JM, Read M, Sutorius E, van Loon JT, Wilkinson MI and Wood PR 2011 The VMC Survey. I. Strategy and first data. *Astron. Astrophys.* **527**, A116.
- Clement CM, Xu X and Muzzin AV 2008 The distance of the first overtone RR Lyrae variables in the MACHO Large Magellanic Cloud database: a new method to correct for the effects of crowding. *Astron. J.* **135**. 83–91.
- Clementini G, Federici L Corsi C, Cacciari C, Bellazzini M and Smith HA 2001 RR Lyrae variables in the globular clusters of M31: a first detection of likely candidates. *Astrophys. J.* **559**, L109–L112.
- Clementini G, Gratton R, Bragaglia A, Carretta E, Di Fabrizio L and Maio M 2003 Distance to the Large Magellanic Cloud: the RR Lyrae stars. *Astron. J.* **125**, 1309–1329.
- Clementini G, Contreras R, Federici L, Cacciari C, Merighi R, Smith HA, Catelan M, Fusi Pecci F, Marconi M, Kinemuchi K and Pritzl BJ 2009 The variable star population of the globular cluster B514 in the Andromeda galaxy. *Astrophys. J.* 704, L103–L107.
- Cole AA 1998 Age, metallicity, and the distance to the Magellanic Clouds from red clump stars. *Astrophys. J.* **500**, L137–L140.
- Costa E, Méndez RA, Pedreros MH, Moyano M, Gallart C, Noël N, Baume G and Carraro G 2009 The proper motion of the Magellanic Clouds. I. First results and description of the program. *Astron. J.* **137**, 4339–4360.
- Dambis AK 2009 The kinematics and zero-point of the log  $P \langle M_K \rangle$  relation for Galactic RR Lyrae variables via statistical parallax. *Mon. Not. R. Astron. Soc.* **396**, 553–569.
- Dambis AK 2010 Estimating the kinematic parameters and the distance-scale zero point for the thindisk, thick-disk, and halo population tracers via 3D velocity data. In *Proc. Variable Stars, the Galactic Halo and Galaxy Formation* (eds Sterken C, Samus N and Szabados L), pp. 177–180. Moscow, Sternberg Astronomical Institute.
- Davis J, Mendez A, Seneta EB, Tango WJ, Booth AJ, O'Byrne JW, Thorvaldson ED, Ausseloos M, Aerts C and Uytterhoeven K 2005 Orbital parameters, masses and distance to β Centauri determined with the Sydney University Stellar Interferometer and high-resolution spectroscopy. *Mon. Not. R. Astron. Soc.* **356**, 1362–1370.
- de Grijs R and Robertson ARI 2006 Arp 116: interacting system or chance alignment? *Astron. Astrophys.* **460**, 493–498.
- Descartes R 1637 Discourse on the Method of Rightly Conducting One's Reason and of Seeking Truth in the Sciences (French original: Discours de la méthode pour bien conduire sa raison, et chercher la vérité dans les sciences). Leiden, Ian Maire Publ.
- de Vaucouleurs G 1993a Tests of the long and short extragalactic distance scales. *Publ. Nat'l Acad. Sci. USA* **90**, 4811–4813.
- de Vaucouleurs G 1993b The extragalactic distance scale. VIII. A comparison of distance scales. *Astrophys. J.* **415**, 10–32.
- Di Benedetto GP 2008 The Cepheid distance to the Large Magellanic Cloud and NGC 4258 by the surface brightness technique and improved calibration of the cosmic distance scale. *Mon. Not. R. Astron. Soc.* **390**, 1762–1776.
- Dopita MA 1992 A theoretical calibration of the planetary nebular cosmic distance scale. *Astrophys. J.* **389**, 27–38.
- Draine BT and Bond NA 2004 Direct extragalactic distance determination using X-ray scattering. *Astrophys. J.* **617**, 987–1003.
- Dunn LP and Jerjen H 2006 First results from SAPAC: toward a three-dimensional picture of the Fornax cluster core. Astron. J. 132, 1384–1395.
- Durrell PR, Harris WE and Pritchet CJ 2001 Photometry and the metallicity distribution of the outer halo of M31. *Astron. J.* **121**, 2557–2571.
- Eckart A and Genzel R 1996 Observations of stellar proper motions near the Galactic Centre. *Nature* **383**, 415–417.
- Eisenhauer F, Schödel R, Genzel R, Ott T, Tecza M, Abuter R, Eckart A and Alexander T 2003 A geometric determination of the distance to the Galactic Center. *Astrophys. J.* **597**, L121–L124.

- Eisenhauer F, Genzel R, Alexander T, Abuter R, Paumard T, Ott T, Gilbert A, Gillessen S, Horrobin M, Trippe S, Bonnet H, Dumas C, Hubin N, Kaufer A, Kissler-Patig M, Monnet G, Ströbele S, Szeifert T, Eckart A, Schödel R and Zucker S 2005 SINFONI in the Galactic Center: young stars and infrared flares in the central light-month. *Astrophys. J.* **628**, 246–259.
- Elitzur M 1992 Astronomical masers. Annu. Rev. Astron. Astrophys. 30, 75–112.
- Filippenko AV 2005 Type Ia supernovae and cosmology. In *White Dwarfs: Cosmological and Galactic Probes* (eds Sion E, Vennes S and Shipman H), *Astrophys. Space Sci. Libr.* **332**, 97–133.
- Fitzpatrick EL, Ribas I, Guinan EF, Maloney FP and Claret A 2003 Fundamental properties and distances of Large Magellanic Cloud eclipsing binaries. IV. HV 5936. Astrophys. J. 587, 685–700.
- Fouqué P, Arriagada P, Storm J, Barnes TG, Nardetto N, Mérand A, Kervella P, Gieren W, Bersier D, Benedict GF and McArthur BE 2007 A new calibration of Galactic Cepheid period–luminosity relations from *B* to *K* bands, and a comparison to LMC relations. *Astron. Astrophys.* **476**, 73–81.
- Frail DA, Diamond PJ, Cordes JM and van Langevelde HJ 1994 Anisotropic scattering of OH/IR stars toward the Galactic Center. *Astrophys. J.* **427**, L43–L46.
- Freedman WL and Madore BF 1991 Metallicity effects on the Cepheid distance scale. In *The Magellanic Clouds* (eds Haynes R and Milne D), *Proc. Int'l Astron. Union Symp.* **148**, 471–472.
- Freedman WL and Madore BF 2010 The Hubble constant. *Annu. Rev. Astron. Astrophys.* **48**, 673–710. Freedman WL, Madore BF, Gibson BK, Ferrarese L, Kelson DD, Sakai S, Mould JR, Kennicutt Jr RC, Ford HC, Graham JA, Huchra JP, Hughes SMG, Illingworth GD, Macri LM, and Stetson PB
- RC, Ford HC, Graham JA, Huchra JP, Hughes SMG, Illingworth GD, Macri LM and Stetson PB 2001 Final results from the Hubble Space Telescope Key Project to measure the Hubble constant. *Astrophys. J.* **553**, 47–72.
- Freire PC, Camilo F, Kramer M, Lorimer DR, Lyne AG, Manchester RN and D'Amico N 2003 Further results from the timing of the millisecond pulsars in 47 Tucanae. *Mon. Not. R. Astron. Soc.* **340**, 1359–1374.
- Frieman JA, Turner MS and Huterer D 2008 Dark energy and the accelerating Universe. *Annu. Rev. Astron. Astrophys.* **46**, 385–432.
- Fritz T, Gillessen S, Trippe S, Ott T, Bartko H, Pfuhl O, Dodds-Eden K, Davies R, Eisenhauer F and Genzel R 2010 What is limiting near-infrared astrometry in the Galactic Centre? *Mon. Not. R. Astron. Soc.* **401**, 1177–1188.
- Gardiner LT and Noguchi M 1996 *N*-body simulations of the Small Magellanic Cloud and the Magellanic Stream. *Mon. Not. R. Astron. Soc.* **278**, 191–208.
- Genzel R, Reid MJ, Moran JM and Downes D 1981 Proper motions and distances of H<sub>2</sub>O maser sources. I. The outflow in Orion-KL. *Astrophys. J.* **244**, 884–902.
- Genzel R, Pichon C, Eckart A, Gerhard OE and Ott T 2000 Stellar dynamics in the Galactic Centre: proper motions and anisotropy. *Mon. Not. R. Astron. Soc.* **317**, 348–374.
- Genzel R, Eisenhauer F and Gillessen S 2010 The Galactic Center massive black hole and nuclear star cluster. *Rev. Mod. Phys.* **82**, 3121–3195.
- Ghez AM, Salim S, Hornstein SD, Tanner A, Lu JR, Morris M, Becklin EE and Duchêne G 2005 Stellar orbits around the Galactic Center black hole. *Astrophys. J.* **620**, 744–757.
- Ghez AM, Salim S, Weinberg NN, Lu JR, Do T, Dunn JK, Matthews K, Morris MR, Yelda S, Becklin EE, Kremenek T, Milosavljevic M and Naiman J 2008 Measuring distance and properties of the Milky Way's central supermassive black hole with stellar orbits. *Astrophys. J.* 689, 1044–1062.
- Gibson BK 2000 The distance to the Large Magellanic Cloud. Mem. Soc. Astron. It. 71, 693-700.
- Gillessen S, Eisenhauer F, Trippe S, Alexander T, Genzel R, Martins F and Ott T 2009a Monitoring stellar orbits around the massive black hole in the Galactic Center. *Astrophys. J.* **692**, 1075–1109.
- Gillessen S, Eisenhauer F, Fritz TK, Bartko H, Dodds-Eden K, Pfuhl O, Ott T and Genzel R 2009b The orbit of the star S2 around Sgr A\* from Very Large Telescope and Keck data. *Astrophys. J.* 707, L114–L117.
- Gould A 2000 A new kinematic distance estimator to the Large Magellanic Cloud. *Astrophys. J.* **528**, 156–160.
- Gould A, Stutz A and Frogel JA 2001 A method to measure the ratio of total to selective extinction toward Baade's Window. *Astrophys. J.* **547**, 590–593.
- Gratton RG, Fusi Pecci F, Carretta E, Clementini G, Corsi CE and Lattanzi M 1997 Ages of globular clusters from Hipparcos parallaxes of local subdwarfs. *Astrophys. J.* 491, 749–771.

- Groenewegen MAT and Blommaert JADL 2005 Mira variables in the OGLE bulge fields. *Astron. Astrophys.* **443**, 143–156.
- Habing HJ 1996 Circumstellar envelopes and asymptotic giant branch stars. *Astron. Astrophys. Rev.* **7.** 97–207.
- Harris WE 1996 A catalog of parameters for globular clusters in the Milky Way. *Astron. J.* **112**, 1487–1488. December 2010 edition, http://physwww.mcmaster.ca/%7Eharris/mwgc.dat, accessed 24 December 2010 (arXiv:1012.3224v1).
- Herrnstein JR, Moran JM, Greenhill LJ, Diamond PJ, Inoue M, Nakai N, Miyoshi M, Henkel C and Riess A 1999 A geometric distance to the galaxy NGC4258 from orbital motions in a nuclear gas disk. *Nature* **400**, 539–541.
- Herschel W 1785 On the construction of the heavens. *Phil. Trans. R. Soc. London* **75**, 213–266. (Reprinted in: Dreyer JLE 1912 *The Scientific Papers of Sir William Herschel* **I**, 223–259, London, UK.)
- Hirota T, Bushimata T, Choi YK, Honma M, Imai H, Iwadate K, Jike T, Kameno S, Kameya O, Kamohara R, Kan-Ya Y, Kawaguchi N, Kijima M, Kim MK, Kobayashi H, Kuji S, Kurayama T, Manabe S, Maruyama K, Matsui M, Matsumoto N, Miyaji T, Nagayama T, Nakagawa A, Nakamura K, Oh CS, Omodaka T, Oyama T, Sakai S, Sasao T, Sato K, Sato M, Shibata KM, Shintani M, Tamura Y, Tsushima M and Yamashita K 2007 Distance to Orion KL measured with VERA. Publ. Astron. Soc. Jpn 59, 897–903.
- Holland S 1998 The distance to the M31 globular cluster system. Astron. J. 115, 1916–1920.
- Horrobin M, Eisenhauer F, Tecza M, Thatte N, Genzel R, Abuter R, Iserlohe C, Schreiber J, Schegerer A, Lutz D, Ott T and Schödel I 2004 The Galactic Center. *Astron. Nachr.* **325**, 120–123.
- Jeffries RD 2007 The distance to the Orion Nebula Cluster. Mon. Not. R. Astron. Soc. 376, 1109–1119.
- Jerjen H 2003 Surface brightness fluctuation distances for dwarf elliptical galaxies in the Fornax cluster. *Astrophys.* **398**, 63–79.
- Jerjen H, Binggeli B and Barazza FD 2004 Distances, metallicities, and ages of dwarf elliptical galaxies in the Virgo cluster from surface brightness fluctuations. *Astron. J.* **127**, 771.
- Jewell PR, Webber JC and Snyder LE 1980 The linear shell diameter of IRC+10011. *Astrophys. J.* **242**, L29–L31.
- Jones BF, Klemola AR and Lin DNC 1994 Proper motion of the Large Magellanic Cloud and the mass of the Galaxy. I. Observational results. Astron. J. 107, 1333–1337.
- Joshi YC, Pandey AK, Narasimha D, Sagar R and Giraud-Héraud Y 2003 Identification of 13 Cepheids and 333 other variables in M31. Astron. Astrophys. 402, 113–123.
- Joshi YC, Narasimha D, Pandey AK and Sagar R 2010 Nainital Microlensing Survey detection of short period Cepheids in the disk of M31. *Astron. Astrophys.* **512**, A66.
- Kallivayalil N, van der Marel RP, Alcock C, Axelrod T, Cook KH, Drake AJ and Geha M 2006a The proper motion of the Large Magellanic Cloud using HST. *Astrophys. J.* **638**, 772–785.
- Kallivayalil N, van der Marel RP and Alcock C 2006b Is the SMC bound to the LMC? The Hubble Space Telescope proper motion of the SMC. *Astrophys. J.* **652**, 1213–1229.
- Kallivayalil N, Besla G, Sanderson R and Alcock C 2009 Revisiting the role of M31 in the dynamical history of the Magellanic Clouds. *Astrophys. J.* **700**, 924–930.
- Kapteyn JC 1922 First attempt at a theory of the arrangement and motion of the sidereal system. *Astrophys. J.* **55**, 302–328.
- Kim MK, Hirota T, Honma M, Kobayashi H, Bushimata T, Choi YK, Imai H, Iwadate K, Jike T, Kameno S, Kameya O, Kamohara R, Kan-Ya Y, Kawaguchi N, Kuji S, Kurayama T, Manabe S, Matsui M, Matsumoto N, Miyaji T, Nagayama T, Nakagawa A, Oh CS, Omodaka T, Oyama T, Sakai S, Sasao T, Sato K, Sato M, Shibata KM, Tamura Y and Yamashita K 2008 SiO maser observations toward Orion-KL with VERA. *Publ. Astron. Soc. Jpn* 60, 991–999.
- Koerwer JF 2009 Large Magellanic Cloud distance and structure from near-infrared red clump observations. Astron. J. 138, 1–6.
- Komatsu E, Dunkley J, Nolta MR, Bennett CL, Gold B, Hinshaw G, Jarosik N, Larson D, Limon M, Page L, Spergel DN, Halpern M, Hill RS, Kogut A, Meyer SS, Tucker GS, Weiland JL, Wollack E and Wright EL 2009 Five-year Wilkinson Microwave Anisotropy Probe observations: cosmological interpretation. *Astrophys. J. Suppl. Ser.* 180, 330–376.

- Komatsu E, Smith KM, Dunkley J, Bennett CL, Gold B, Hinshaw G, Jarosik N, Larson D, Nolta MR, Page L, Spergel DN, Halpern M, Hill RS, Kogut A, Limon M, Meyer SS, Odegard N, Tucker GS, Weiland JL, Wollack E and Wright EL 2011 Seven-year Wilkinson Microwave Anisotropy Probe (WMAP) observations: cosmological interpretation. *Astrophys. J. Suppl. Ser.* **192**, 18.
- Kraus S, Balega YY, Berger J-P, Hofmann K-H, Millan-Gabet R, Monnier JD, Ohnaka K, Pedretti E, Preibisch T, Schertl D, Schloerb FP, Traub WA and Weigelt G 2007 Visual/infrared interferometry of Orion Trapezium stars: preliminary dynamical orbit and aperture synthesis imaging of the  $\theta^1$  Orionis C system. *Astron. Astrophys.* **466**, 649–659.
- Kroupa P and Bastian U 1997 The Hipparcos proper motion of the Magellanic Clouds. *New Astron.* **2**, 77–90
- Kroupa P, Röser S and Bastian U 1994 On the motion of the Magellanic Clouds. *Mon. Not. R. Astron. Soc.* **266**, 412–420.
- Kunder A and Chaboyer B 2008 Metallicity analysis of MACHO Galactic bulge RR0 Lyrae stars from their light curves. *Astron. J.* **136**, 2441–2452.
- Lazio TJW, Anantharamaiah KR, Goss WM, Kassim NE and Cordes JM 1999 G359.87+0.18, an FR II radio galaxy 15' from Sagittarius A\*: implications for the scattering region in the Galactic Center. *Astrophys. J.* **515**, 196–205.
- Lindblad B 1927 On the nature of the spiral nebulae. Mon. Not. R. Astron. Soc. 87, 420-426.
- Lindqvist M, Winnberg A, Johansson LEB and Ukita N 1991 SiO maser emission from OH/IR stars close to the Galactic Centre. *Astron. Astrophys.* **250**, 431–436.
- Liu MC and Graham JR 2001 Infrared surface brightness fluctuations of the Coma elliptical galaxy NGC 4874 and the value of the Hubble constant. *Astrophys. J.* **557**, L31–L34.
- Lo KY 2005 Mega-masers and galaxies. Annu. Rev. Astron. Astrophys. 43, 625-676.
- Lo KY, Cohen MH, Readhead ASC and Backer DC 1981 Multiwavelength VLBI observations of the Galactic Center. *Astrophys. J.* **249**, 504–512.
- Macri LM, Stanek KZ, Bersier D, Greenhill LJ and Reid MJ 2006 A new Cepheid distance to the maser-host galaxy NGC 4258 and its implications for the Hubble constant. *Astrophys. J.* **652**, 1133–1149.
- Majaess DJ 2010 Concerning the distance to the center of the Milky Way and its structure. *Acta Astron.* **60**, 55–74.
- Majaess DJ, Turner DG and Lane DJ 2009 Characteristics of the Galaxy according to Cepheids. *Mon. Not. R. Astron. Soc.* **398**, 263–270.
- Majaess D, Turner D and Lane D 2010 Type II Cepheids as extragalactic distance candles. *Acta Astron.* **59**, 403–418.
- Massey P, Armandroff TE, Pyke R, Patel K and Wilson CD 1995 Hot, luminous stars in selected regions of NGC 6822, M31, and M33. *Astron. J.* **110**, 2715–2738.
- Matsunaga N, Kawadu T, Nishiyama S, Nagayama T, Hatano H, Tamura M, Glass IS and Nagata T 2009 A near-infrared survey of Miras and the distance to the Galactic Centre. *Mon. Not. R. Astron. Soc.* **399**, 1709–1729.
- McConnachie AW, Irwin MJ, Ferguson AMN, Ibata RA, Lewis GF and Tanvir N 2005 Distances and metallicities for 17 Local Group galaxies. *Mon. Not. R. Astron. Soc.* **356**, 979–997.
- McNamara DH, Madsen JB, Barnes J and Ericksen BF 2000 The distance to the Galactic Center. *Publ. Astron. Soc. Pac.* **112**, 202–216.
- Mei S, Blakeslee JP, Tonry JL, Jordán A, Peng EW, Côté P, Ferrarese L, West MJ, Merritt D and Milosavljević M 2005 The Advanced Camera for Surveys Virgo Cluster Survey. V. Surface brightness fluctuation calibration for giant and dwarf early-type galaxies. Astrophys. J. 625, 121–129.
- Mei S, Blakeslee JP, Côté P, Tonry JL, West MJ, Ferrarese L, Jordán A, Peng EW, Anthony A and Merritt D 2007 The ACS Virgo Cluster Survey. XIII. SBF distance catalog and the three-dimensional structure of the Virgo cluster. *Astrophys. J.* **655**, 144–162.
- Menten KM, Reid MJ, Eckart A and Genzel R 1997 The position of Sagittarius A\*: accurate alignment of the radio and infrared reference frames at the Galactic Center. *Astrophys. J.* **475**, L111–L114.
- Menten KM, Reid MJ, Forbrich J and Brunthaler A 2007 The distance to the Orion Nebula. *Astron. Astrophys.* 474, 515–520.

- Messineo M, Habing HJ, Sjouwerman LO, Omont A and Menten KM 2002 86 GHz SiO maser survey of late-type stars in the inner Galaxy. I. Observational data. *Astron. Astrophys.* **393**, 115–128.
- Messineo M, Habing HJ, Menten KM, Omont A and Sjouwerman LO 2004 86 GHz SiO maser survey of late-type stars in the inner Galaxy. II. Infrared photometry of the SiO target stars. *Astron. Astrophys.* 418, 103–116.
- Muir J 1911 My First Summer in the Sierra. Houghton Mifflin Co.
- Nemec JM, Nemec AFL and Lutz TE 1994 Period–luminosity–metallicity relations, pulsation modes, absolute magnitudes, and distances for Population 2 variable stars. *Astron. J.* **108**, 222–246.
- Ngeow C and Kanbur SM 2008 Large Magellanic Cloud distance from Cepheid variables using least squares solutions. In *Proc. Galaxies in the Local Volume* (eds Koribalski BS and Jerjen H), *Astrophys. Space Sci. Proc.*, pp. 317–318.
- Nishiyama S, Nagata T, Sato S, Kato D, Nagayama T, Kusakabe N, Matsunaga N, Naoi T, Sugitani K and Tamura M 2006 The distance to the Galactic Center derived from infrared photometry of bulge red clump stars. *Astrophys. J.* **647**, 1093–1098.
- Olling RP 2007 Accurate extragalactic distances and dark energy: anchoring the distance scale with rotational parallaxes. *Mon. Not. R. Astron. Soc.* **378**, 1385–1399.
- Olling RP and Peterson DM 2000 One percent distances to Local Group galaxies via rotational parallaxes. *Bull. Am. Astron. Soc.* **32**, 1576–1576.
- Oort JH 1927 Observational evidence confirming Lindblad's hypothesis of a rotation of the galactic system. *Bull. Astron. Inst. Neth.* **3**, 275–282.
- Pedreros MH, Anguita C and Maza J 2002 Proper motion of the Large Magellanic Cloud using QSOs as an inertial reference system: the Q0459-6427 field. Astron. J. 123, 1971-1977.
- Perlmutter S, Aldering G, Goldhaber G, Knop RA, Nugent P, Castro PG, Deustua S, Fabbro S, Goobar A, Groom DE, Hook IM, Kim AG, Kim MY, Lee JC, Nunes NJ, Pain R, Pennypacker CR, Quimby R, Lidman C, Ellis RS, Irwin M, McMahon RG, Ruiz-Lapuente P, Walton N, Schaefer B, Boyle BJ, Filippenko AV, Matheson T, Fruchter AS, Panagia N, Newberg HJM, Couch WJ and the Supernova Cosmology Project 1999 Measurements of Ω and Λ from 42 high-redshift supernovae. *Astrophys. J.* **517**, 565–586.
- Peterson D and Shao M 1997 The scientific basis for the Space Interferometry Mission. In *Proc. ESA Symp. Hipparcos Venice '97* (ed. Perryman MAC), *ESA Spec. Publ.* **402**, pp. 749–754.
- Piatek S, Pryor C and Olszewski EW 2008 Proper motions of the Large Magellanic Cloud and Small Magellanic Cloud: re-analysis of Hubble Space Telescope data. *Astron. J.* **135**, 1024–1038.
- Pietrzyński G, Thompson IB, Graczyk D, Gieren W, Udalski A, Szewczyk O, Minniti D, Kołaczkowski Z, Bresolin F and Kudritzki R-P 2009 The Araucaria project. Determination of the Large Magellanic Cloud distance from late-type eclipsing binary systems. I. OGLE-051019.64—685812.3. *Astrophys. J.* **697**, 862–866.
- Press WH, Flannery BP, Teukolsky SA and Vetterling WT 1992 Kolmogorov–Smirnov test. In *Numerical Recipes in Fortran 77: The Art of Scientific Computing*, 2nd edn, pp. 617–622. Cambridge University Press.
- Reid MJ 1993 The distance to the center of the Galaxy. *Annu. Rev. Astron. Astrophys.* **31**, 345–372. Reid MJ and Brunthaler A 2004 The proper motion of Sagittarius A\*. II. The mass of Sagittarius A\*. *Astrophys. J.* **616**, 872–884.
- Reid MJ, Schneps MH, Moran JM, Gwinn CR, Genzel R, Downes D and Rönnäng B 1988 The distance to the center of the Galaxy: H<sub>2</sub>O maser proper motions in Sagittarius B2(N). *Astrophys. J.* **330**, 809–816.
- Reid MJ, Readhead ACS, Vermeulen RC and Treuhaft RN 1999 The proper motion of Sagittarius A\*. I. First VLBA results. *Astrophys. J.* **524**, 816–823.
- Reid MJ, Menten KM, Genzel R, Ott T, Schödel R and Eckart A 2003 The position of Sagittarius A\*. II. Accurate positions and proper motions of stellar SiO masers near the Galactic Center. *Astrophys. J.* **587**, 208–220.
- Reid MJ, Menten KM, Zheng XW, Brunthaler A, Moscadelli L, Xu Y, Zhang B, Sato M, Honma M, Hirota T, Hachisuka K, Choi YK, Moellenbrock GA and Bartkiewicz A 2009a Trigonometric parallaxes of massive star-forming regions. VI. Galactic structure, fundamental parameters, and noncircular motions. *Astrophys. J.* 700, 137–148.

- Reid MJ, Menten KM, Zheng XW, Brunthaler A and Xu Y 2009b A trigonometric parallax of Sgr B2. *Astrophys. J.* **705**, 1548–1553.
- Reid WA and Parker QA 2010 A new population of planetary nebulae discovered in the Large Magellanic Cloud, III. The luminosity function, *Mon. Not. R. Astron. Soc.* 405, 1349–1374.
- Ribas I, Jordi C, Vilardell F, Fitzpatrick EL, Hilditch RW and Guinan EF 2005 First determination of the distance and fundamental properties of an eclipsing binary in the Andromeda galaxy. *Astrophys. J.* **635**, L37–L40.
- Riess AG, Filippenko AV, Challis P, Clocchiatti A, Diercks A, Garnavich PM, Gilliland RL, Hogan CJ, Jha S, Kirshner RP, Leibundgut B, Phillips MM, Reiss D, Schmidt BP, Schommer RA, Smith RC, Spyromilio J, Stubbs C, Suntzeff NB and Tonry J 1998 Observational evidence from supernovae for an accelerating Universe and a cosmological constant. *Astron. J.* 116, 1009–1038.
- Riess AG, Macri L, Casertano S, Sosey M, Lampeitl H, Ferguson HC, Filippenko AV, Jha SW, Li W, Chornock R and Sarkar D 2009a A redetermination of the Hubble constant with the Hubble Space Telescope from a differential distance ladder. *Astrophys. J.* **699**, 539–563.
- Riess AG, Macri L, Li W, Lampeitl H, Casertano S, Ferguson HC, Filippenko AV, Jha SW, Chornock R, Greenhill L, Mutchler M, Ganeshalingham M and Hicken M 2009b Cepheid calibrations of modern Type Ia supernovae: implications for the Hubble constant. *Astrophys. J. Suppl. Ser.* 183, 109–141.
- Ruffle PME, Zijlstra AA, Walsh JR, Gray MD, Gesicki K, Minniti D and Comeron F 2004 Angular diameters, fluxes and extinction of compact planetary nebulae: further evidence for steeper extinction towards the bulge. *Mon. Not. R. Astron. Soc.* 353, 796–812.
- Růžička A, Theis C and Palouš J 2009 Spatial motion of the Magellanic Clouds: tidal models ruled out? Astrophys. J. 691, 1807–1815.
- Salim S and Gould A 1999 Sagittarius A\* 'visual binaries': a direct measurement of the Galactocentric distance. *Astrophys. J.* **523**, 633–641.
- Sandage A, Tammann GA, Saha A, Reindl B, Macchetto FD and Panagia N 2006 The Hubble constant: a summary of the Hubble Space Telescope program for the luminosity calibration of Type Ia supernovae by means of Cepheids. *Astrophys. J.* **653**, 843–860.
- Sandage A, Tammann GA and Reindl B 2009 New period–luminosity and period–color relations of classical Cepheids. III. Cepheids in SMC. Astron. Astrophys. 493, 471–479.
- Sandstrom KM, Peek JEG, Bower GC, Bolatto AD and Plambeck RL 2007 A parallactic distance of 389<sup>+24</sup><sub>-21</sub> parsecs to the Orion Nebula Cluster from Very Long Baseline Array observations. *Astrophys. J.* **667**, 1161–1169.
- Sarajedini A, Mancone CL, Lauer TR, Dressler A, Freedman W, Trager SC, Grillmair C and Mighell KJ 2009 RR Lyrae variables in two fields in the spheroid of M31. *Astron. J.* **138**, 184–195.
- Saviane I, Momany Y, da Costa GS, Rich RM and Hibbard JE 2008 A new red giant-based distance modulus of 13.3 Mpc to the Antennae galaxies and its consequences. *Astrophys. J.* **678**, 179–186.
- Schaefer BE 2008 A problem with the clustering of recent measures of the distance to the Large Magellanic Cloud. *Astron. J.* **135**, 112–119.
- Schödel R, Ott T, Genzel R, Hofmann R, Lehnert M, Eckart A, Mouawad N, Alexander T, Reid MJ, Lenzen R, Hartung M, Lacombe F, Rouan D, Gendron E, Rousset G, Lagrange A-M, Brandner W, Ageorges N, Lidman C, Moorwood AFM, Spyromilio J, Hubin N and Menten KM 2002 A star in a 15.2-year orbit around the supermassive black hole at the centre of the Milky Way. *Nature* 419, 694–696.
- Schultz GV, Sherwood WA and Winnberg A 1978 Radial diameters of type II OH/IR sources. *Astron. Astrophys.* **63**, L5–L7.
- Schweizer F, Burns CR, Madore BF, Mager VA, Phillips MM, Freedman WL, Boldt L, Contreras C, Folatelli G, González S, Hamuy M, Krzeminski W, Morrell NI, Persson SE, Roth MR and Stritzinger MD 2008 A new distance to the Antennae galaxies (NGC 4038/39) based on the type Ia supernova 2007sr. *Astron. J.* **136**, 1482–1489.
- Shapley H 1918a Studies based on the colors and magnitudes in stellar clusters. Seventh paper: The distances, distribution in space, and dimensions of 69 globular clusters. *Contrib. Mount Wilson Obs.* **152**, 1–28.

- Shapley H 1918b Studies based on the colors and magnitudes in stellar clusters. VII. The distances, distribution in space, and dimensions of 69 globular clusters. *Astrophys. J.* **48**, 154–181.
- Shaya EJ and Olling R 2009 Rotational parallax: a SIM science study. *Bull. Am. Astron. Soc.* 41, 356–356.
- Sjouwerman LO, van Langevelde HJ and Diamond PJ 1998 Stellar positions from SiO masers in the Galactic Center. *Astron. Astrophys.* **339**, 897–903.
- Sjouwerman LO, Lindqvist M, van Langevelde HJ and Diamond PJ 2002 H<sub>2</sub>O and SiO maser emission in Galactic Center OH/IR stars. *Astron. Astrophys.* **391**, 967–978.
- Sjouwerman LO, Messineo M and Habing HJ 2004 43 GHz SiO masers and astrometry with VERA in the Galactic Center. *Publ. Astron. Soc. Jpn* **56**, 45–50.
- Snyder LE, Kuan Y-J and Miao Y 1994 Where is the heavy molecule Heimat in Sgr B2? In *Proc. The Structure and Content of Molecular Clouds* (eds Wilson TJ and Johnston KJ), *Lect. Notes Phys.* **439**, 187–198.
- Solanes JM, Sanchis T, Salvador-Solé E, Giovanelli R and Haynes MP 2002 The three-dimensional structure of the Virgo cluster region from Tully–Fisher and HI data. *Astron. J.* **124**, 2440–2452.
- Sollima A, Cacciari C, Arkharov AAH, Larionov VM, Gorshanov DL, Efimova NV and Piersimoni A 2008 The infrared *JHK* light curves of RR Lyr. *Mon. Not. R. Astron. Soc.* **384**, 1583–1587.
- Stanek KZ and Garnavich PM 1998 Distance to M31 with the Hubble Space Telescope and Hipparcos red clump stars. *Astrophys. J.* **503**, L131–L134.
- Szewczyk O, Pietrzyński G, Gieren W, Storm J, Walker A, Rizzi L, Kinemuchi K, Bresolin F, Kudritzki R-P and Dall'Ora M 2008 The Araucaria project. The distance of the Large Magellanic Cloud from near-infrared photometry of RR Lyrae variables. *Astron. J.* **136**, 272–279.
- Tammann GA, Sandage A and Reindl B 2003 New period–luminosity and period–color relations of classical Cepheids. I. Cepheids in the Galaxy. Astron. Astrophys. 404, 423–448.
- Tonry JL, Blakeslee JP, Ajhar EA and Dressler A 2000 The surface brightness fluctuation survey of galaxy distances. II. Local and large-scale flows. *Astrophys. J.* **530**, 625–651.
- Trippe S, Gillessen S, Gerhard OE, Bartko H, Fritz TK, Maness HL, Eisenhauer F, Martins F, Ott T, Dodds-Eden K and Genzel R 2008 Kinematics of the old stellar population at the Galactic Centre. *Astron. Astrophys.* **492**, 419–439.
- Trumpler RJ 1930 Preliminary results on the distances, dimensions and space distribution of open star clusters. *Lick Obs. Bull.* XIV, 154–188.
- Udalski A 2003 The Optical Gravitational Lensing Experiment: is interstellar extinction toward the Galactic Center anomalous? *Astrophys. J.* **590**, 284–290.
- Vanhollebeke E, Groenewegen MAT and Girardi L 2009 Stellar populations in the Galactic bulge. Modelling the Galactic bulge with TRILEGAL. *Astron. Astrophys.* **498**, 95–107.
- van Langevelde HJ and Diamond PJ 1991 Interstellar scattering of OH/IR stars at the Galactic Centre. *Mon. Not. R. Astron. Soc.* **249**, 7P–10P.
- van Leeuwen F, Feast MW, Whitelock PA and Laney CD 2007 Cepheid parallaxes and the Hubble constant. *Mon. Not. R. Astron. Soc.* **379**, 723–737.
- Vilardell F, Ribas I and Jordi C 2006 Eclipsing binaries suitable for distance determination in the Andromeda galaxy. *Astron. Astrophys.* **459**, 321–331.
- Vilardell, F, Jordi C and Ribas I 2007 A comprehensive study of Cepheid variables in the Andromeda galaxy. Period distribution, blending, and distance determination. Astron. Astrophys. 473, 847–855.
- Vilardell F, Ribas I, Jordi C, Fitzpatrick EL and Guinan EF 2010 The distance to the Andromeda galaxy from eclipsing binaries. Astron. Astrophys. 509, A70.
- von Struve FGW 1847 Etudes d'astronomie stellaire: sur la voie lactée et sur la distance des etoiles fixes. IV. St. Petersburg, Tip. Acad. Imper.
- Walker AR 2003 Distances to Local Group galaxies. In *Proc. Stellar Candles for the Extragalactic Distance Scale* (eds Alloin D and Gieren W), *Lect. Notes Phys.* **635**, 265–279.
- West MJ and Blakeslee JP 2000 The principal axis of the Virgo cluster. *Astrophys. J.* **543**, L27–L30. Westerlund BE 1997 The Magellanic Clouds. *Cambridge Astrophys. Ser.* **29**.
- Yusef-Zadeh F, Hewitt JW and Cotton W 2004 A 20 centimeter survey of the Galactic Center region. I. Detection of numerous linear filaments. *Astrophys. J. Suppl. Ser.* **155**, 421–550.